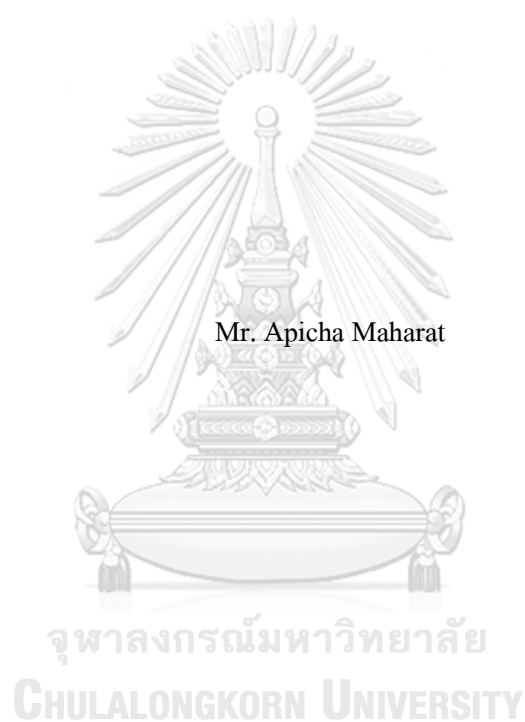FORMALDEHYDE FLUORESCENT SENSORS FROM 1,8-NAPHTHALIMIDE
DERIVATIVES

Mr. Apicha Maharat

A Thesis Submitted in Partial Fulfillment of the Requirements

for the Degree of Master of Science in Petrochemistry and Polymer Science

Field of Study of Petrochemistry and Polymer Science

FACULTY OF SCIENCE

Chulalongkorn University

Academic Year 2019

ฟลูออเรสเซนต์เซนเซอร์สำหรับฟอร์มัลดีไฮด์จากอนุพันธ์1,8-แนฟธาลิไมด์

นายอภิชา มหารัตน์

วิทยานิพนธ์นี้เป็นส่วนหนึ่งของการศึกษาตามหลักสูตรปริญญาวิทยาศาสตรมหาบัณฑิต
สาขาวิชาปิโตรเคมีและวิทยาศาสตร์พอลิเมอร์ สาขาวิชาปิโตรเคมีและวิทยาศาสตร์พอลิเมอร์
คณะวิทยาศาสตร์ จุฬาลงกรณ์มหาวิทยาลัย
ปีการศึกษา 2562
ลิขสิทธิ์ของจุฬาลงกรณ์มหาวิทยาลัย

Thesis Title   FORMALDEHYDE FLUORESCENT SENSORS FROM 1,8-

        NAPHTHALIMIDE DERIVATIVES

By   Mr. Apicha Maharat

Field of Study   Petrochemistry and Polymer Science

Thesis Advisor   Associate Professor Dr. PAITOON RASHATASAKHON

Accepted by the FACULTY OF SCIENCE, Chulalongkorn University in Partial Fulfillment of the Requirement for the Master of Science

            Dean of the FACULTY OF SCIENCE

   (Professor Dr. POLKIT SANGVANICH)

THESIS COMMITTEE

            Chairman

   (Assistant Professor Dr. WARINTHORN CHAVASIRI)

            Thesis Advisor

   (Associate Professor Dr. PAITOON RASHATASAKHON)

            Examiner

   (Associate Professor Dr. SIRILUX POOMPRADUB)

            External Examiner

   (Assistant Professor Dr. Vachiraporn Ajavakom)

อภิชา มหารัตน์ : ฟลูออเรสเซนต์เซนเซอร์สำหรับฟอร์มัลดีไฮด์จากอนุพันธ์1,8-แนฟธาลิไมด์. (FORMALDEHYDE FLUORESCENT SENSORS FROM 1,8-NAPHTHALIMIDE DERIVATIVES) อ.ที่ปรึกษาหลัก : รศ. ดร.ไพฑูรย์ รัชตะสาคร

การออกแบบและสังเคราะห์อนุพันธ์ของแนพธาลิไมด์สามชุด สำหรับตรวจสอบผลของหมู่แทนที่ต่อสมบัติเชิงแสงและตรวจวัดฟอร์มาลดีไฮด์ในตัวกลางที่เป็นน้ำ หมู่แทนที่สำคัญคือ ไฮดราซีน (-NHNH$_2$) และ 2-เมทอกซีเอทิลลามีน (-NHCH$_2$CH$_2$OCH$_3$) ติดตั้งไปที่ตำแหน่งที่ 4 ของแนพธาลิไมด์ผ่านปฏิกิริยาการแทนที่ด้วยสารนิวคลีโอไฟล์ และปฏิกิริยาการควบแน่น ได้ผลผลิตร้อยละ 60–80% อนุพันธ์ของแนพธาลิไมด์ ที่มีหมู่แทนที่เป็นไฮดราซีน 2 หมู่ (R3) สามารถตรวจวัดฟอร์มาลดีไฮด์ได้อย่างจำเพาะเจาะจง มีการเพิ่มขึ้นของสัญญาณฟลูออเรสเซนต์ที่ความยาวคลื่น 520 นาโนเมตร 3.5 เท่า ในสารละลายกรดอะซีติก 5% กลไกการตรวจวัดฟอร์มาลดีไฮด์เกี่ยวข้องกับการยับยั้งกระบวนการถ่ายโอนอิเล็กตรอนที่ถูกเหนี่ยวนำด้วยแสง (PET) ระหว่างไฮดราซีนและแนพธาลิไมด์โดยฟอร์มาลดีไฮด์ ให้ค่าต่ำสุดที่สามารถ ตรวจวัดได้ (LOD) คือ 0.1 มิลลิโมลาร์ ซึ่งต่ำกว่าค่าที่องค์การอนามัยโลก กำหนดไว้สำหรับสารฟอร์มาลดีไฮด์ในน้ำดื่ม ไม่เกิน 0.33 มิลลิโมลาร์ สำหรับแอลดีไฮด์อื่นๆ และสารที่เกี่ยวข้อง อีก 11 ชนิดไม่รบกวนการตรวจวัดฟอร์มาลดีไฮด์อย่างมีนัยสำคัญ นอกจากนี้ความไวการตรวจวัดของ R3 ต่อฟอร์มาลดีไฮด์ ยังเพิ่มขึ้นจากการทำหมู่แทนที่ไฮดราซีนให้อยู่ในรูปกรด โดยใช้ก๊าซไฮโดรเจนคลอไรด์ อีกทั้งยังสามารถขึ้นรูป R3.HCl ใน ซิลิกาโซลเจลที่มีความเข้มข้นของ R3.HCl 10 ไมโครโมลาร์ สามารถตรวจวัดฟอร์มาลดีไฮด์ที่ความเข้มเข้มข้น 2 ถึง 0.02 ไมโครโมลาร์ ได้ด้วยตาเปล่า

สาขาวิชา	ปิโตรเคมีและวิทยาศาสตร์พอลิเมอร์	ลายมือชื่อนิสิต ....
ปีการศึกษา	2562	ลายมือชื่อ อ.ที่ปรึกษาหลัก ....

6072156823 : MAJOR PETROCHEMISTRY AND POLYMER SCIENCE

KEYWORD: NAPHTHALIMIDE / FORMALDEHYDE / FLUORESCENCE SENSOR

Apicha Maharat : FORMALDEHYDE FLUORESCENT SENSORS FROM 1,8-NAPHTHALIMIDE DERIVATIVES . Advisor: Assoc. Prof. Dr. PAITOON RASHATASAKHON

Three derivatives of 1,8-naphthalimide were systematically designed and synthesized to investigate the effect of substitution pattern on their photophysical properties and sensing behaviors towards formaldehyde in aqueous media. The key substituents, the hydrazino ($-NHNH_2$) and the 2-methoxyethylamino groups ($-NHCH_2CH_2OCH_3$), were installed at the 4-position of 1,8-naphthalimide by a nucleophilic replacement, and at the imide position by a condensation reaction with 1,8-naphthalic anhydride precursor. All target compounds were obtained in good overall yields of 60-80%. Compounds with two hydrazine moieties (R3) showed excellent selective fluorescent responses towards formaldehyde with the 3.5-fold fluorescence enhancement in 5% aqueous acetic acid solution at 520 nm. The sensing mechanism likely involves the inhibition of photo-induced electron transfer (PET) between the hydrazine and naphthalimide moieties by formaldehyde. The detection limit of the R3 probe was calculated to be 0.1 mM. Other aldehydes and related analysts did not show significant interference in the fluorescence spectrum. Moreover, the sensitivity of the R3 probe toward formaldehyde was successfully enhanced by protonation of the hydrazine moiety with HCl gas to give R3.HCl. The fabrication of R3.HCl in sol-gel was successfully demonstrated. The doping of 10 µM of R3.HCl in silica sol-gel led to a sensor which was capable of formaldehyde detection at 2 to 0.02 µM by naked eyes.

| Field of Study: | Petrochemistry and Polymer Science | Student's Signature .... |
| Academic Year: | 2019 | Advisor's Signature .... |

ACKNOWLEDGEMENTS

TABLE OF CONTENTS

LIST OF TABLES

LIST OF FIGURES

จุฬาลงกรณ์มหาวิทยาลัย
CHULALONGKORN **U**NIVERSITY

LIST OF SCHEMES

จุฬาลงกรณ์มหาวิทยาลัย

CHULALONGKORN UNIVERSITY

LIST OF ABBREVIATIONS

calcd	calculated
^{13}C NMR	carbon-13 nuclear magnetic resonance
CDCl$_3$	deuterated chloroform
CH$_2$Cl$_2$	dichloromethane
CH$_3$CN	Acetonitrile
DMSO-d_6	deuterated dimethyl sulfoxide
EtOAc	ethyl acetate
equiv	equivalent (s)
g	gram (s)
HOMO	highest occupied molecular orbital
^{1}H NMR	proton nuclear magnetic resonance
Hz	Hertz
h	hour (s)
J	coupling constant
LUMO	lowest unoccupied molecular orbital
MALDI-TOF MS	matrix assisted laser desorption/ionization-time of flight mass spectrometry
m	multiplet (NMR)
MeOH	methanol

mg	milligram (s)
mL	milliliter (s)
mmol	millimole (s)
m/z	mass per charge ratio
M.W.	molecular weight
M	molar
MHz	megahertz
nm	nanometer
rt	room temperature
s	singlet (NMR)
THF	tetrahydrofuran
TLC	thin layer chromatography
UV	ultraviolet
v/v	volume by volume
δ	chemical shift
ε	molar extinction coefficient
λ	wavelength
°C	degree Celsius
μL	microliter (s)
μM	micromolar (s)
Φ	quantum yield

% yield   percentage yield

CHAPTER I

INTRODUCTION

1.1 Overview

Formaldehyde (FA) is a common air pollutant at ambient temperature. It is known as formalin in liquid form when prepared at 35–40% in aqueous solution with methanol as a stabilizer. It is widely used in several applications such as household products [1], cosmetics [2],and drug [[3]. Formalin has also been used to extend shelf-life in seafood and vegetables, while several research indicate that FA is a toxic and carcinogenic substance for human [4], and it can cause multitudinous diseases such as allergies [5], brain infarction [6], and headache [7]. General techniques such as high-performance liquid chromatography (HPLC) [8], gas chromatography (GC) [9], mass spectrophotometry (MS) [10], and quartz crystal microbalance (QCM) [11] have been used for the analysis of FA. Although these techniques can provide outstanding sensitivity and precision, they require expensive instrument costs, well-trained technicians, and complicated operational procedure. To overcome these limitations, the fluorescent technique has been introduced and applied as an analytical technique due to its high sensitivity and selectivity with the simple instrument operation.

1.2 Fluorescence

Fluorescence is a member of the luminescence phenomena, which involve the absorption of electromagnetic or electrical energy and emission of light from an excited molecule to the ground state. The mechanism of fluorescence phenomenon can be illustrated using a Jablonski diagram [12] **(Figure 1.1)**. The first transition in Jablonski diagrams is the absorption of particular energy by the molecule, which then convert from its ground to the excited state. The excited molecules are generally unstable in these higher electronic states (S_1, S_2 or higher), and they will eventually dissipate the energy and return to the ground state through a non-radiative transition such as internal conversion (IC), intersystem crossing (ISC) and vibrational relaxation. The release of the remaining energy will occur in the form of fluorescence light when the molecule return to ground state.
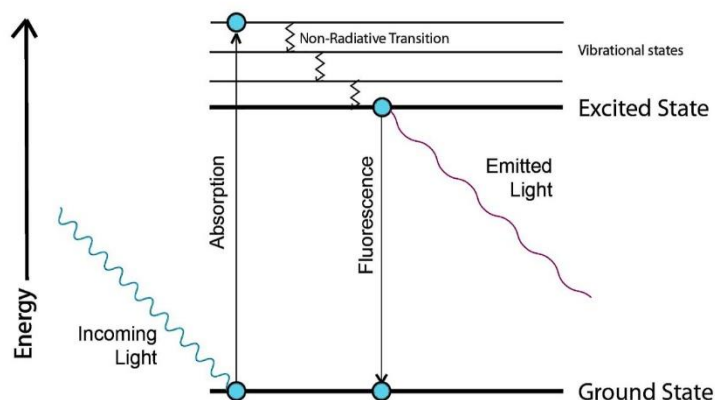
Figure1.1 Jablonski diagram

Typical fluorescence compounds usually derive from aromatic molecules. Widely used fluorophores are xanthene dyes like fluorescein and rhodamine. The emission spectra are dependent on the chemical structure of the fluorophore and the chemical environment in which it is dissolved or immobilized. By looking at the Jablonsky diagram in more detail, one can see that the energy of the emission is less than that of absorption.

Consequently, the fluorescence emission band is shifted to longer wavelengths in comparison to the absorption band. The difference in the band maxima positions of absorption and emission spectra is known as Stokes shift. Regarding the optical sensing application, massive stokes shifts are advantageous since excitation and emission wavelengths can be fully separated which allows the detection of only the emission intensity without interference with the excitation source intensity. Other specific characteristics of a fluorophore are lifetime and quantum yield. Quantum yield is the number of emitted photons relative to the number of absorbed photons. Molecules like rhodamines have large quantum yields and thus display bright emissions. The fluorescence lifetime mentions to the average time the fluorophore stays in its excited state before emitting a photon. It determines the time available for the molecule to interact with its environment and hence, the information to read out from its emission.

1.3 Fluorescence chemosensors and mechanism

Over the past decade, fluorescent sensors are used for detection of several analytes in chemical, biological, and environmental research. Fluorescence chemosensors are usually composed of a reporter, a signaling unit, and a spacer or linker **(Figure 1.2).** When a sensor

interacts with a specific analyte, which results in a change of fluorescence intensity, intensity decay, or a shift of the emission wavelength. The mechanism which controls the response of a fluorophore to analyte binding includes photo-induced electron transfer (PET), internal charge transfer (ICT), fluorescence resonance energy transfer (FRET), excited-state intramolecular proton transfer (ESIPT), structural isomerization, aggregation-induced enhancement fluorescence (AIE), and aggregation-caused quenching (ACQ). In addition, more than one mechanism can be used to design sensor.
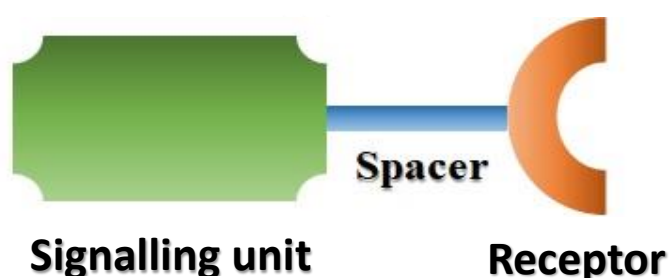
Figure 1.2 The component of fluorescent chemosensors

1.3.1 Photo-induced electron transfer (PET)

Photo-induced electron transfer (PET) is a mechanism that has been widely used in the design fluorescence sensor [13] **(Figure 1.3)**. When an electron of the fluorophore is excited from the Highest Occupied Molecular Orbital (HOMO) to Lowest Unoccupied Molecular Orbital (LUMO), the electron from HOMO of the receptor which has higher energy will transfer to the HOMO of the fluorophore, resulting in a fluorescent signal decrease or fluorescence turn-off. However, when there is a binding between receptor and analyte, making the energy level of HOMO of the receptor lower than the fluorophore, resulting in electron from receptor cannot transfer to a fluorophore. Therefore, the fluorescent signal will be significantly increased, and it is called a fluorescence turn-on **(Figure 1.4)**.
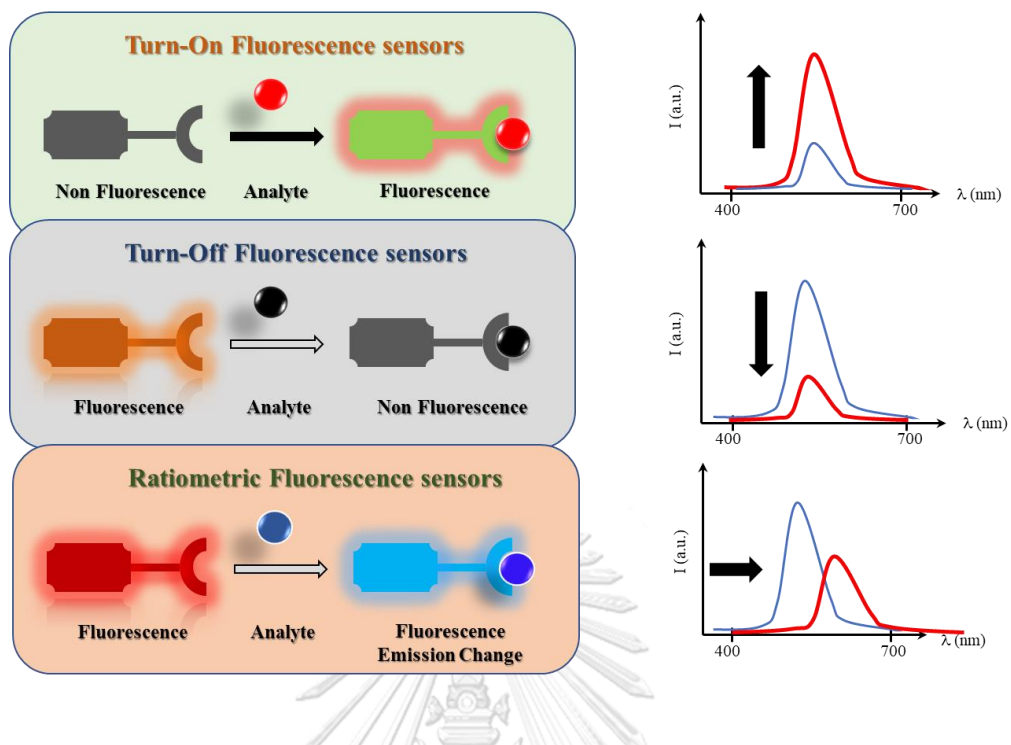
Figure 1.3 Modes of Photo-induced electron transfer (PET)
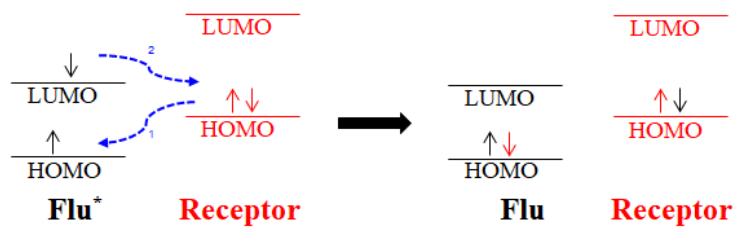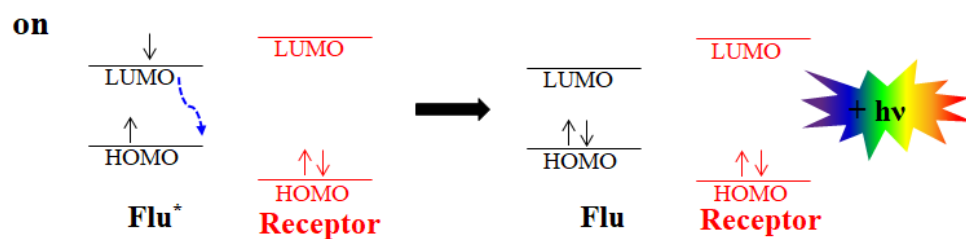
Figure 1.4 Photo-induced electron transfer (PET) effect

1.3.2 Internal charge transfer (ICT)

The electron delocalization process may occur in a substance whose structure consists of an electron-donating and electron-withdrawing groups. This process is known as the internal charge transfer (ICT) [14]. The molecule at the locally excited state (LE) can adapt into a more stable ICT state following the Frank-Condon principle. This state has lower energy and different geometry from the LE state. The fluorescence intensity will be lower and a large stoke shift occurred which is called "red shift". After ICT state relaxes to ground state the molecule may give light within or outside the visible light spectrum (**Figure 1.5**).
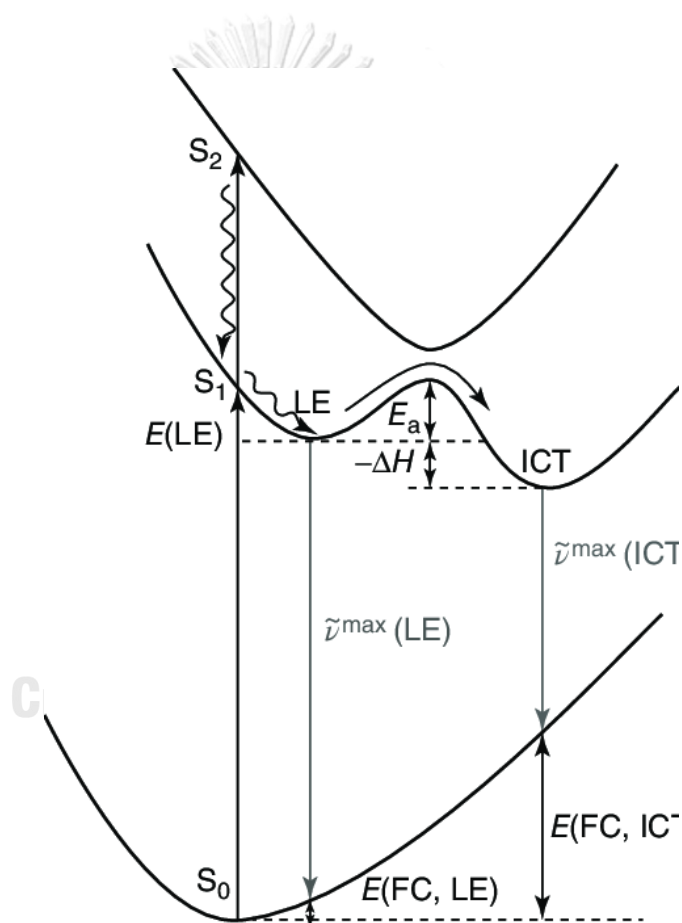
Figure 1.5 Principle of the ICT quenching mechanism

1.4 Fluorescence sensor for formaldehyde

1.4.1 Introduction of a fluorescence sensor for formaldehyde

For the detection of formaldehyde by fluorescence, two mechanisms of measurement have been reported. They involve either a 2-aza-Cope rearrangement, or condensation of formaldehyde to formimine or methylene hydrazines [15]. (**Figure 1.6**)
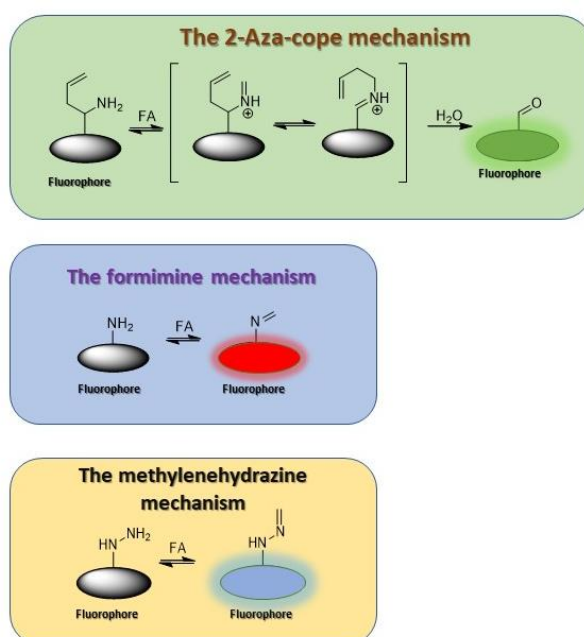
Figure 1.6 Mechanisms for formaldehyde detection.

1.4.2 Literature review on the 2-aza-cope rearrangement reaction

The 2-aza-cope rearrangement mechanism is a reaction between formaldehyde and homoallylic amine, to generate aldehyde or ketone product by undergoes the 2-aza-cope rearrangement and hydrolyzes. This mechanism exhibits good selectivity for formaldehyde over other reactive carbonyl species such as acetaldehyde, 4-hydroxynonenal and methylglyoxal. The change on conversion of a homoallylamine to a carbonyl can cause a fluorescence turn-on or ratio change.

In 2015, Chang et al. [16] develop and synthesized the fluorescent probe based on 2-aza-cope rearrangement reaction. Probe FAP-1 is weakly fluorescent at first, but when it treatment with 100 µM formaldehyde, It showed about 8-fold fluorescence turn-on response (λ_{max} = 645 nm, λ_{em} = 662 nm) **(Figure 1.7)**.
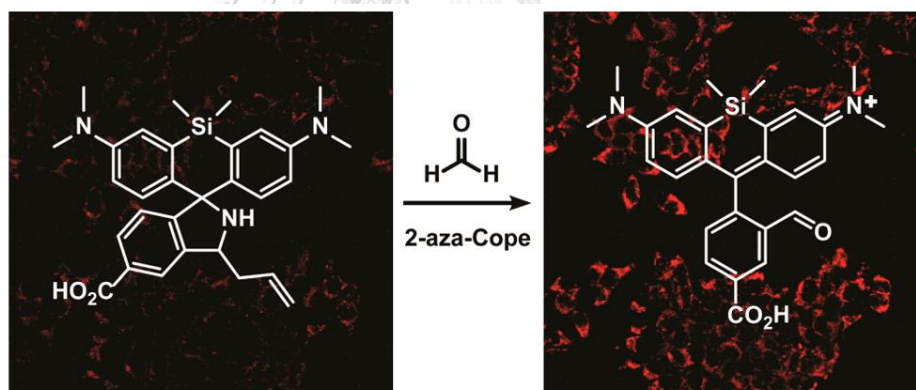
Figure 1.7 Structure of FAP-1 and its fluorescent response to formaldehyde.

1.4.3 Literature review on the condensation reaction of Free amino

Alternative approaches for formaldehyde detection by use the properties between formaldehyde and free amines. The free amines probes affected in the electron transfer due to the existence of lone pair electrons on amino group. The condensation of the amino group with formaldehyde lead to a constraint of electron transfer which resulting in the turn-on fluorescence.

In 2012, Yoon et al. [17] was design and synthesized fluorescence probe for formaldehyde by attach BODIPY dye to amine group. Probe showed weak fluorescence since the electron transfer from the free amine moiety to the BODIPY fluorophore quenched the fluorophore. Nonetheless, the addition of formaldehyde in CH_3OH at pH 8 induced a strong green emission at 535 nm upon excitation at 520 nm (**Figure 1.8**).
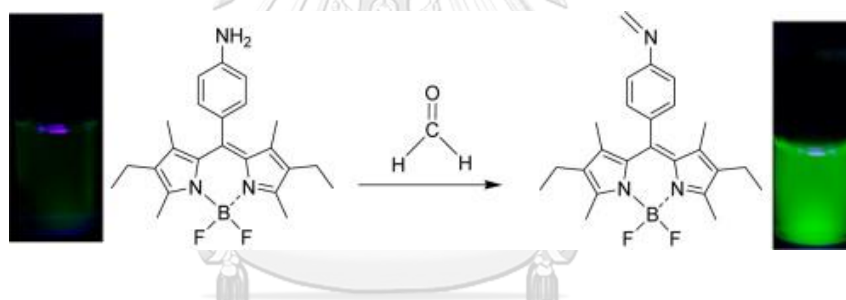
Figure 1.8 Structure of BODIPY derivative and its fluorescent response toward formaldehyde.

1.4.4 Literature review on the condensation reaction of hydrazine

Similar, the hydrazine also compose of amino group like the free amino. which can also react with formaldehyde to produce the methylenehydrazine.

In 2016, Kim et al., [18] reported probe x which is contain 1,8-naphthalimide as a fluorophore and hydrazine as a reaction part **(Figure 1.9)**. In the beginning, probe 1 had PET process and low fluorescence properties. The fluorophore displayed a strong fluorescence turn-on at 541 nm in response to formaldehyde in a outstanding 〜140-fold fluorescence enhancement.
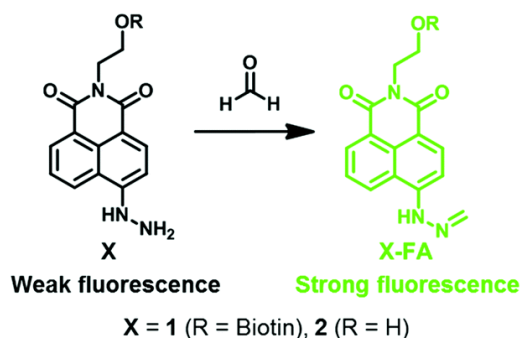
Figure 1.9 Structure of probe x and product (X-FA) upon adding formaldehyde.

1.5 Fluorescence sensor base on naphthalimide

1.5.1 Introduction of naphthalimide

Derivatives of 1,8-naphthalimide are relevant aromatic heterocycles. The core structure of naphthalimide is shown in **Figure 1.10**. They have been widely applied as fluorescence dyes [19], colourants, organic light-emitting materials, antitumor, anti-inflammatory, antidepressant, cytotoxic agents, DNA binder and antiviral agents. Due to their excellent fluorescence properties, high absorption coefficients, good fluorescence and quantum yields, large stokes shifts, excellent stability and easy modification. Which these advantages, in the past, there have many reports that use naphthalimide as fluorescent sensors.
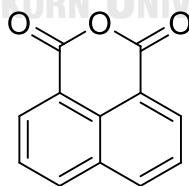
Figure 1.10 The core structure of naphthalimide

1.5.2 Literature review on 1,8-naphthalimide derivatives based fluorescence sensors toward formaldehyde

2015, Dong et al. [20] reported probe NPz containing hydrazine as a binding unit and use naphthalimide as the fluorophore for formaldehyde detection **(Figure1.11)**. At the initial state, it had PET process and low fluorescence properties. After addition of formaldehyde in 5% acetic acid, The PET process was suppressed and The ICT process appeared. Probe NPz brought the strong emission at 540 nm showing a detection limit ca 0.25 ppm.
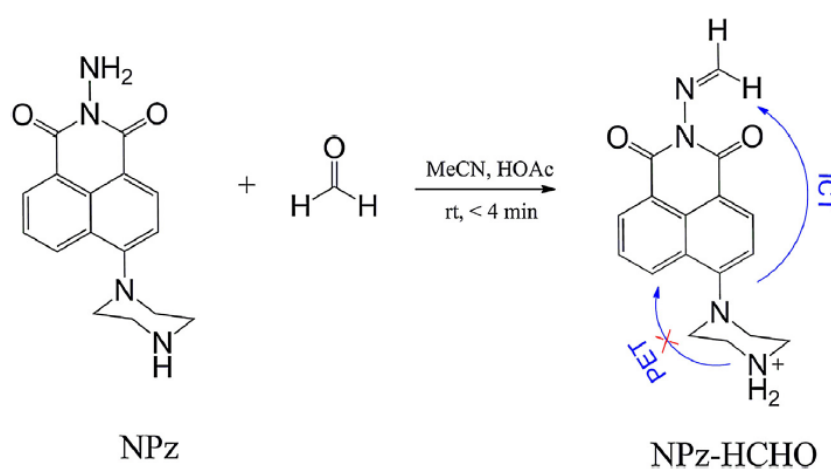
Figure 1.11 Structure of probe NPz and product (NPz-HCHO) upon adding formaldehyde.

In 2016, Tang et al. [21] develop and synthesized the fluorescent probe based on naphthalimide and hydrazine **(Figure 1.12)**. In addition, it also contains morpholine moiety that design to attaches on lysosome make these dye can visualize the endogenous formaldehyde in the lysosomes in living cells.
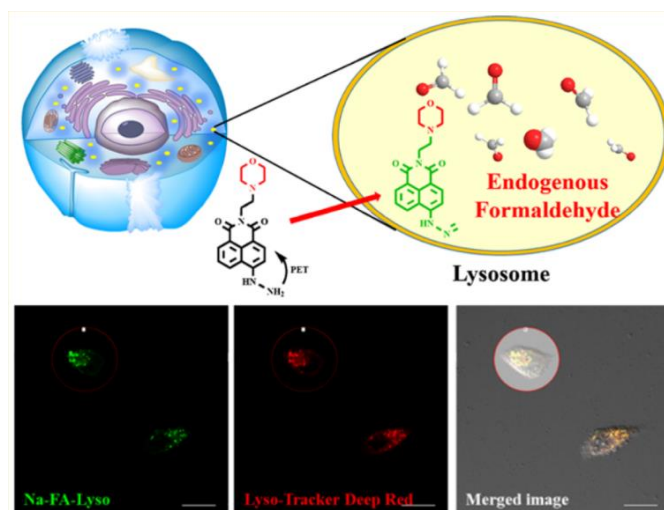
Figure 1.12 Fluorescence Response Mechanism of the Lysosome‑Targetable FA Probe Na‑FA‑Lyso and Fluorescence imaging.

Recently, in 2017, Bi et al., successfully design and synthesized probe for formaldehyde based on acylation reaction of hydrazine **(Figure 1.13)**. The fluorophore exhibited a strong fluorescence turn‑on at 525 nm in response to formaldehyde in aqueous media. The turn‑on signal results from the conversion of hydrazine to generate methylenehydrazine product. The detection limit of the probe was determined as low as 20 nM. It is the lowest limits for FA detection. Furthermore, the probe could detect formaldehyde within 5 miniute in aqueous solution.
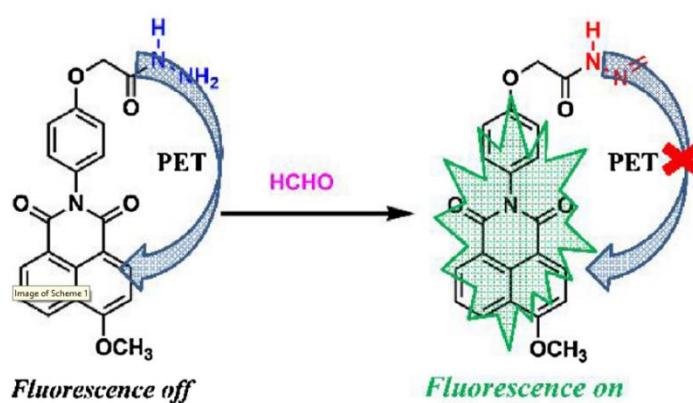
Figure 1.13 Structure of sensor and product upon adding formaldehyde.

1.6 Sol gel in fluorescence sensing

The sol-gel process is a suitable method to synthesize xerogel films or aerogels from silicon alkoxide precursors **(Figure 1.14)**. In a first step, the precursors, commonly tetraethoxysilane (TEOS) is spread in methanol or ethanol forming a sol. Upon addition of water and a base or an acid, the silicon alkoxide precursors ($Si(OR)_4$) are hydrolyzed (eq. 1) and finally condensed to form siloxane bridges (eq. 2 and eq.3) [22]. At this stage, the solvent can be evaporated at room or elevated temperature, or the sol is first allowed to condense forming a gel, as shown in **Figure 1.14**. Solvent evaporation typically causes shrinkage since the solvent leaves the micropores of the silica network. Evaporation of the solvent at the sol stage leads to more short films, whereas the evaporation at the gel stage can lead to more porous ceramics since the previous gelation has formed a silica network. Alternatively, removal of the solvent by supercritical drying of the gel leads to a material which is similar in the size and shape of the original gel. The resulting aerogel has low solid volume fractions near 1% and thus very high pore volumes.

Hydrolysis: $Si(OR)_4 + xH_2O \; HO_x\text{-}Si(OR)_{4-x} + xROH$ (eq 1)

Condensation: $(RO)_3Si\text{-}OH + HO\text{-}Si(OR)_3 \; (RO)_3Si\text{-}O\text{-}Si(OR)_3 + H_2O$ (eq 2)

And/or $(RO)_3Si\text{-}OR + HO\text{-}Si(OR)_3 \; (RO)_3Si\text{-}O\text{-}Si(OR)_3 + ROH$ (eq 3)
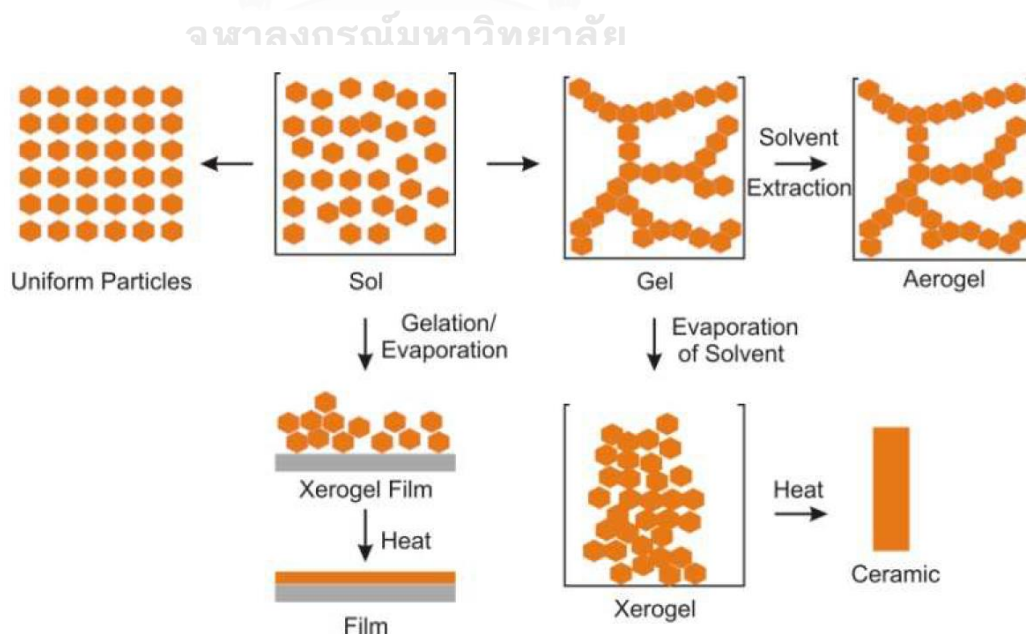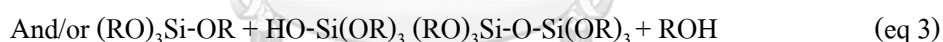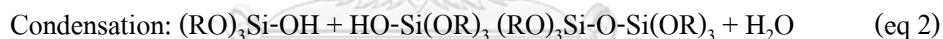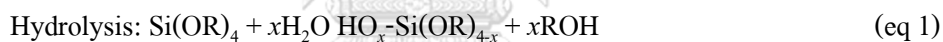
Figure 1.14 Overview of the sol gel process.

Process parameters such as pH, ratio of water to silicon alkoxide precursor, drying conditions and solvent contribute to the properties of the silica films. Sol-gel materials offer several advantages for the fluorescence sensing application including optical transparency from the ultraviolet to infrared wavelengths, process versatility that facilitates tailoring of the film properties (e.g. porosity, refractive index, polarity, elasticity) as well as chemical and thermal stability. Another benefit of the sol-gel process is the possibility of simple chemical doping of the material by adding the desired dye molecules to the precursor sol solution. Upon polymerization of the precursors, the dyes are immobilized into the silica matrix. Organically modified silica (Ormosil) based sol-gels offer several advantages for sensing compared to purely inorganic sol-gels. The enhanced hydrophobicity improves the sensitivity of the sensor. Furthermore, the more rigid networks (due to the lower degree of cross-linking) of ormosil xerogels are reported to positively impact the photo-degradation of the dye molecules resulting in less photo-bleaching of the dyes.
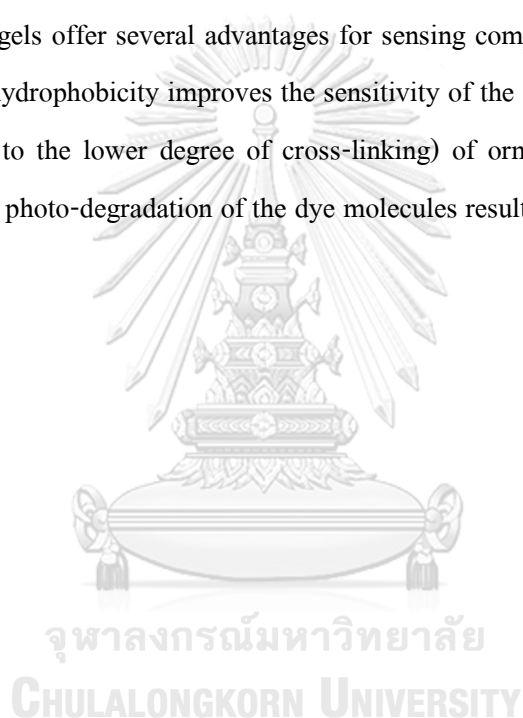
1.7 Objective and expected outcome of this work

In this research, three fluorescence chemosensors based on naphthalimide derivatives (**R1-R3**) containing the hydrazino (-NHNH$_2$) as a receptor unit and the 2-methoxyethylamino groups (-NHCH$_2$CH$_2$OCH$_3$) are designed and synthesized (**Figure 1.15**). The photophysical and sensing properties will be thoroughly investigated. When the hydrazine moiety reacts with formaldehyde, an enhanced fluorescence signals should be observed as the PET process will be prohibited. In addition, the fabrication of these sensors in silica sol-gel will be carried out in order to obtain a portable sensor kit for the detection of formaldehyde.
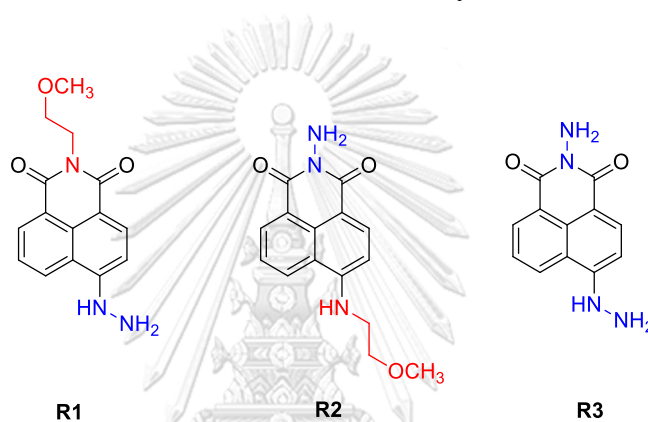
Figure 1.15 Target molecules

CHAPTER II

EXPERIMENTAL

2.1 Chemicals and materials

2-Methoxyethylamine and hydrazine monohydrate, acetylacetone, and ammonium acetate were purchased from Sigma-Aldrich. 4-Bromo-1,8-naphthalic anhydride was purchased from Chemieliva Phamaceutical Co., Ltd (China). For most reactions, solvents such as methylene chloride (CH_2Cl_2), acetic acid (AcOH), and ethanol (EtOH) were reagent grade and used without purification. Solvents used for extraction and chromatography such as CH_2Cl_2, hexane, EtOAc and MeOH were commercial grade. All column chromatography was operated using Merck silica gel 60 (70-230 mesh). Thin layer chromatography (TLC) was performed on Kieselgel F-254 precoated aluminum TLC plates. Milli-Q water was used in all experiments unless specified otherwise. All reactions were carried out in sealed tube purged with N_2 before and after the introduction of stating materials and solvent.

2.2 Analytical Instruments

The ^{1}H NMR was acquired on Varian Mercury NMR spectrophotometer (Varian, USA) at 400 MHz with chemical shifts reported as ppm in DMSO-d_6. The ^{13}C NMR was measured on Bruker Mercury NMR spectrophotometer (Bruker, Germany, which equipped at 100 MHz with chemical shifts reported as ppm in DMSO-d_6. The UV-visible absorption was performed on a Varian Cary 50 UV-Vis spectrophotometer (Varian, USA) and the fluorescence emission was acquired by Carry Eclipse Fluorescence Spectrophotometer (Agilent Technologies, USA). The HRMS spectra were measured on an electrospray ionization mass spectrometer (MicroTOF, Bruker daltonics, USA).

2.3 Synthesis of R1, R2 and R3

2.3.1 Preparation of 6-bromo-2-(2-methoxyethyl)-1H-benzo[*de*]isoquinoline-1,3(2H)-dione (1)
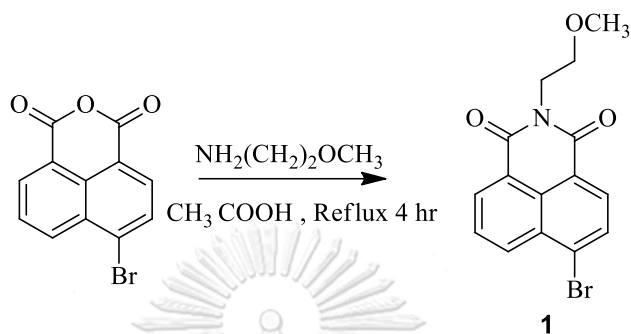
Scheme 2.1 Synthesis of **(1)**

A mixture of 4-bromo-1,8-naphthalic anhydride (5 g, 18.04 mmol), 2-methoxyethylamine (3.14 mL, 36.08 mmol), and glacial acetic acid (50 mL) was refluxed for 4 hours. After the reaction was completed as monitored by TLC, the mixture was allowed to cool to room temperature. The resulting brown precipitate was filtered, washed with copious amount of water and cold ethanol. After vacuum drying for overnight, the crude product was purified by column chromatography on silica gel using 30 % ethyl acetate in hexane as the eluent to afford product 6-bromo-2-(2-methoxyethyl)-1*H*-benzo[*de*]isoquinoline-1,3(2*H*)-dione (**1**) as a yellow solid in 94% yield. ^{1}H NMR (400 MHz, CDCl$_3$) δ 8.69 (d, J = 7.3 Hz, 1H), δ 8.61 (d, J = 7.5 Hz, 1H), δ 8.55 (d, J = 8.4 Hz, 1H), δ 8.13 (d, J = 7.5 Hz, 1H), δ 7.95 (t, J = 7.9 Hz, 1H), δ 4.42 (t, J = 5.7 Hz, 2H), δ 3.73 (t, J = 5.7 Hz, 2H), δ 3.34 (s, 3H). This data is in good agreement with the reported literature [23].

2.3.2 Preparation of 6-hydrazinyl-2-(2-methoxyethyl)-1H-benzo[*de*]isoquinoline-1,3(2H)-dione (R1)
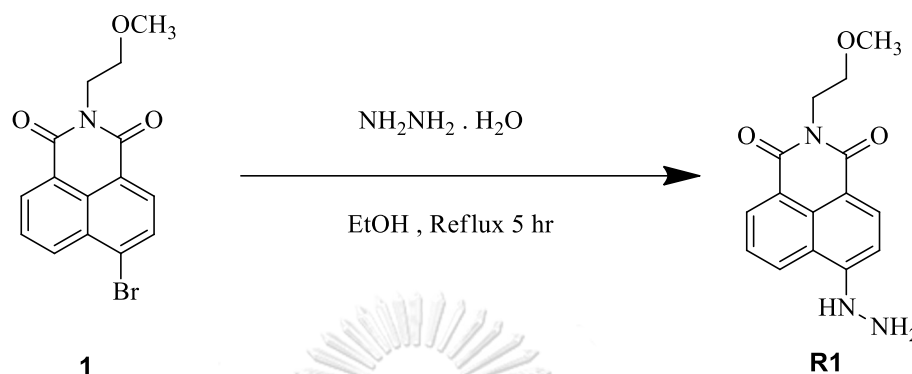
Scheme 2.2 Synthesis of **R1**

A mixture of 6-bromo-2-(2-methoxyethyl)-1H-benzo[de]isoquinoline-1,3(2H)-dione from the previous step, 80% hydrazine hydrate (2.32 mL, 47.84 mmol), and ethanol (40 mL) was stirred and refluxed for 5 h. After cooling to room temperature, the precipitates were filtered and recrystallized from ethanol to afford **R1** as an orange solid. The compound was further purified by column chromatography on silica gel using 30 % ethyl acetate in hexane as the eluent to afford **R1** as an orange solid in 87% yield. ^{1}H NMR (400 MHz, DMSO-d_6) δ 9.10 (s, 1H, -*NH*), 8.56 (d, J =7.7 Hz, 1H, -C$^7_{aro}$*H*), 8.36 (d, J = 7.7 Hz, 1H, -C$^2_{aro}$*H*), 8.24 (d, J = 8.5 Hz, 1H, -C$^5_{aro}$*H*), 7.59 (t, J = 7.7 Hz, 1H, -C$^6_{aro}$*H*), 7.21 (d, J = 8.5 Hz, 1H, -C$^3_{aro}$*H*), 4.67 (s, 2H, -*NH$_2$*), 4.19 (t, J = 6.2 Hz, 2H, -*OCH$_2$*), 3.55 (t, J = 6.2 Hz, 2H, -*NCH$_2$*), 3.25 (s, 3H, -*OCH$_3$*); ^{13}C NMR (100 MHz, DMSO-d_6) δ 163.7, 162.8, 153.1, 134.1, 130.5, 129.2, 128.2, 123.9, 121.5, 118.3, 107.3, 103.9, 68.8, 57.9, 38.1. MS (MALDI-TOF) Calcd for $C_{15}H_{15}N_3NaO_3$: 308.1011; Found: 308.1001.

2.3.3 Preparation of 2-amino-6-bromo-1H-benzo[*de*]isoquinoline-1,3(2H)-dione (2)
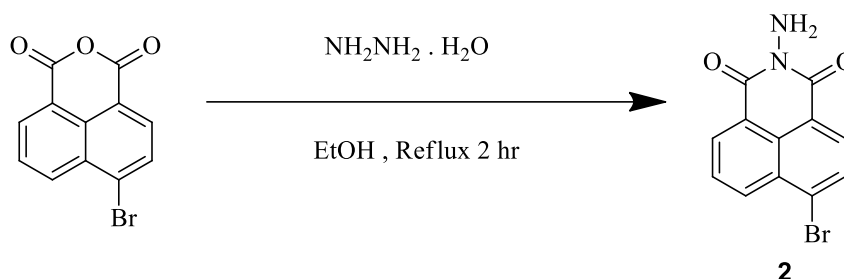
Scheme 2.3 Synthesis of **(2)**

A mixture of 4-bromo-1,8-naphthalic anhydride (1.00 g, 3.61 mmol), 80% hydrazine hydrate (0.70 mL, 14.4 mmol), and ethanol (10 mL) was stirred under reflux for 2 h. After cooling to room temperature, the resulting solid was filtered, washed with water, and dried under vacuum to obtain 2-amino-6-bromo-1H-benzo[*de*]isoquinoline-1,3(2H)-dione (2) in 95% yield. ^{1}H NMR (500 MHz, DMSO-d_6) δ 8.53 (d, $J = 7.2$ Hz, 1H, -C$^7_{aro}H$), 8.48 (d, $J = 7.2$ Hz, 1H, -C$^5_{aro}H$), 8.28 (d, $J = 7.8$ Hz, 1H, -C$^2_{aro}H$), 8.16 (t, $J = 7.2$ Hz, 1H, -C$^6_{aro}H$), 7.95 (d, $J = 7.8$ Hz, 1H, -C$^3_{aro}H$), 5.79 (s, 2H, -NNH_2)); ^{13}C NMR (126 MHz, DMSO-d_6) δ 159.97, 159.93, 132.71, 131.60, 131.39, 130.95, 129.73, 129.28, 128.84, 126.96, 122.41, 121.64.

2.3.4 Preparation of 2-amino-6-((2-methoxyethyl)amino)-1H-benzo[*de*]isoquinoline-1,3(2H)-dione (R2)
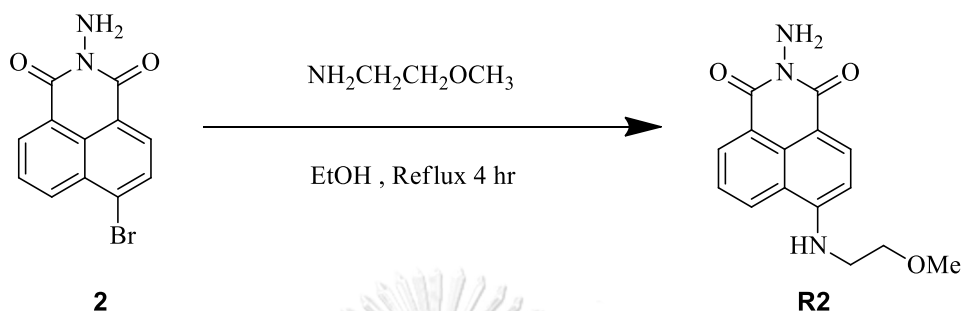
Scheme 2.4 Synthesis of **R2**

A mixture of **2** (0.99 g, 3.4 mmol), 2-methoxyethylamine (0.90 mL, 10.3 mmol), and glacial acetic acid 10 mL was heated under reflux for 4 h. After the reaction was completed and allowed to cool to room temperature, a portion of CH_2Cl_2 (50 mL) was added, and the organic phase was washed with DI water. The organic phase was then dried over anhydrous Na_2SO_4 and concentrated under reduced pressure. The residue was purified by column chromatography using a mixture of hexane/ethyl acetate (1:1, v/v) as the eluent to give **R2** as a light brown solid in 60% yield. ^{1}H NMR (400 MHz, DMSO-d_6) δ 8.69 (d, J = 7.9 Hz, -C$^7_{aro}$*H*), 8.43 (d, J = 7.9 Hz, 1H, -C$^5_{aro}$*H*), 8.24 (d, J = 8.6 Hz, 1H, -C$^2_{aro}$*H*), 7.85 (t, J = 5.1 Hz, 1H, -*NH*), 7.68 (t, J = 7.9 Hz, 1H, -C$^6_{aro}$*H*), 6.81 (d, J = 8.6 Hz, -C$^3_{aro}$*H*), 5.73 (s, 2H, -*NH$_2$*), 3.63 (t, J = 5.1 Hz, 2H, -*OCH$_2$*), 3.58 (t, J = 5.0 Hz, 2H, -*NCH$_2$*). 3.30 (s, 3H, -*OCH3*); ^{13}C NMR (100 MHz, DMSO-d_6) 160.1, 159.9, 150.8, 134.1, 130.4, 128.4, 127.8, 124.1, 121.2, 120.0, 107.1, 103.8, 69.7, 58.1, 42.6. MS (MALDI-TOF) Calcd for $C_{15}H_{15}N_3NaO_3$: 308.1011; Found: 308.1006.

2.3.5 Preparation of 2-amino-6-hydrazinyl-1H-benzo[*de*]isoquinoline-1,3(2H)-dione (R3)
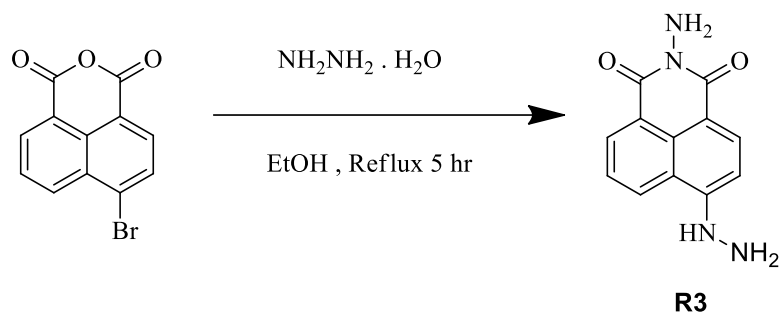
Scheme 2.5 Synthesis of **R3**

A mixture of 4-bromo-1,8-naphthalic anhydride (1.00 g, 3.61 mmol), hydrazine hydrate (0.88 mL, 18.04 mmol), and ethanol (10 mL) was heated under reflux for 5 h. After cooling to room temperature, the precipitates were filtered, washed with water, dried under vacuum. The crude product was recrystallized twice using ethanol to afford **R3** as an orange solid in 90% yield. The ^{1}H-NMR spectrum of this compound was in good agreement with the literature report [24]. ^{1}H NMR (400 MHz, DMSO-d_6) δ 9.20 (s, 1H, -*NH*), 8.62 (d, J = 7.5 Hz, 1H, -C$^7_{aro}$*H*), 8.42 (d, J = 7.5 Hz, 1H, -C$^5_{aro}$*H*), 8.28 (d, J = 8.7 Hz, 1H, -C$^2_{aro}$*H*), 7.64 (t, J = 7.5 Hz, 1H, -C$^6_{aro}$*H*), 7.24 (d, J = 8.7 Hz, 1H, -C$^3_{aro}$*H*), 5.72 (s, 2H, -*NNH$_2$*), 4.69 (s, 2H, -*NHNH$_2$*); ^{13}C NMR (126 MHz, DMSO-d_6) δ 160.2, 160.1, 153.6, 134.4, 130.6, 128.3, 127.9, 124.2, 121.3, 118.5, 106.7, 104.2. MS (MALDI-TOF) Calcd for $C_{12}H_{10}N_4NaO_2$: 265.0701; Found: 265.0695.

2.4 Photophysical properties

The stock solutions of **R1**-**R3** in DMSO were prepared at 1 mM and diluted to desired

concentrations for spectrophotometric experiments.

2.4.1 UV‑Visible spectroscopy

All UV‑Visible absorption spectra were recorded from 400 nm to 800 nm at ambient

temperature.

2.4.1.1 The molar extinction coefficient ($\mathbf{\mathcal{E}}$)

The molar extinction coefficient ($\mathbf{\mathcal{E}}$) of each fluorophore were calculated from the UV

absorption spectra in DMSO at various concentrations. The absorbances at the maximum

absorption wavelengths (A) of each compound were plotted against the concentrations (C) at the

respective excitation wavelengths. Each plot should be a straight line goes through the origin. The

molar extinction coefficient ($\mathbf{\mathcal{E}}$) represented into the following equation:

$$A = \mathbf{\mathcal{E}}bC$$

*b is the cell path length.

2.4.2 Fluorescence spectroscopy

The stock solutions of **R1**-**R3** were diluted to 10 μM in 1% DMSO and 99% Water. The

emission spectra of fluorophore were recorded from 400 nm to 800 nm at ambient temperature

using an excitation wavelength at 410, 435 and 410 nm, respectively.

2.4.3 Fluorescence quantum yield

The fluorescence quantum yield of fluorophores were perform in DMSO by using

quinine sulfate ($\mathbf{\Phi}_{F}$ = 0.54 in 0.1 N H_2SO_4) as the standard reference. The UV‑Visible absorption

spectra of samples and reference at five different concentrations (A < 0.1) were recorded. The

fluorescence emission spectra of the same set of solutions using appropriate excitation

wavelengths selected were recorded based on the absorption maximum wavelength (λ_{max}) of each

compound. Graphs of integrated fluorescence intensity were plotted against the absorbance at the

respective excitation wavelengths. Each plot should be straight line with an intercept at 1 and a slope or gradient *m*. In addition, the fluorescence intensity vs. absorbance represented into the following equation.

$$\Phi_X = \Phi_{ST}\left(\frac{Grad_x}{Grad_{ST}}\right)\left(\frac{\eta_x^2}{\eta_{ST}^2}\right)$$

The subscripts Φ_{ST} denote the fluorescence quantum yield of standard reference which used quinine sulfate ($\Phi = 0.54$ in 0.1 N H_2SO_4) and Φ_X is the fluorescence quantum yield of sample and η is the refractive index of the solvent.

2.5 Fluorescent sensor study

The stock solutions of **R1-R3** in DMSO were prepared at 1 mM and diluted to desired concentrations for spectrophotometric experiments.

2.5.1 Formaldehyde sensing

The stock solutions of formaldehyde in DI water was prepared at 10 mM and diluted to desired concentrations for spectrophotometric experiments.

2.5.1.1 Selectivity screening

Stock solution of each fluorophore (1 mM) were prepared in DMSO. Several aldehyde samples such as formaldehyde, terephathaldehyde, naphthaldehyde, 3-methoxybenzaldehyde, 2-nitrobenzaldehyde, propionaldehyde, acetaldehyde, valeradehyde, and nonanal were also prepared in DMSO at 10 mM. The stock solutions of sensors (**R1-R3**) and analytes (aldehyde samples) were diluted with 5% acetic acid solution in water to achieve the final concentration of **R1-R3** at 10 μM and 1 mM respectively.

2.5.1.2 Interference test

Fluorescence response of **R1**-**R3** (10 µM) in the presence of formaldehyde (100 µM) and interfering compounds (1 mM) were recorded under the same instrument conditions. These experiments will allow a selectivity assessment of these sensors.

2.5.1.3 Detection limit

The limit of detection was estimated by plotting of fluorescence change of **R3** in the range of formaldehyde concentration 0.1-1.0 mM. The detection limit is then calculated with the equation: detection limit = $3\sigma/m$, where σ is the standard deviation of blank measurements; m is the slope from a linear plot between intensity versus sample concentration.

2.5.1.4 Effect of solvent

The stock solutions are diluted into 10 µM by varied solvents including, EtOH, THF, CH_3CN, Water and DMSO. The emission spectra of fluorophores with and without analyte were recorded at room temperature using an excitation wavelength.

2.5.1.5 Effect of water content

The stock solutions are diluted into 10 µM by varied water content between 0% - 99% water in DMSO. The emission spectra of fluorophores with and analyte were recorded at room temperature using an excitation wavelength.

CHAPTER III

Results and Discussion

Fluorescent targets R1-R3

3.1 Synthesis and characterization

According to our molecular design, 1,8-naphthalimide was used as a fluorophore and hydrazine unit was installed as a receptor for formaldehyde. The synthetic routes of these target compounds are shown in **Scheme 3.1**. The different substitution position of the hydrazine and the hydrophilic 2-methoxyethyl group in **R1** and **R2** could lead to different sensitivity towards formaldehyde detection
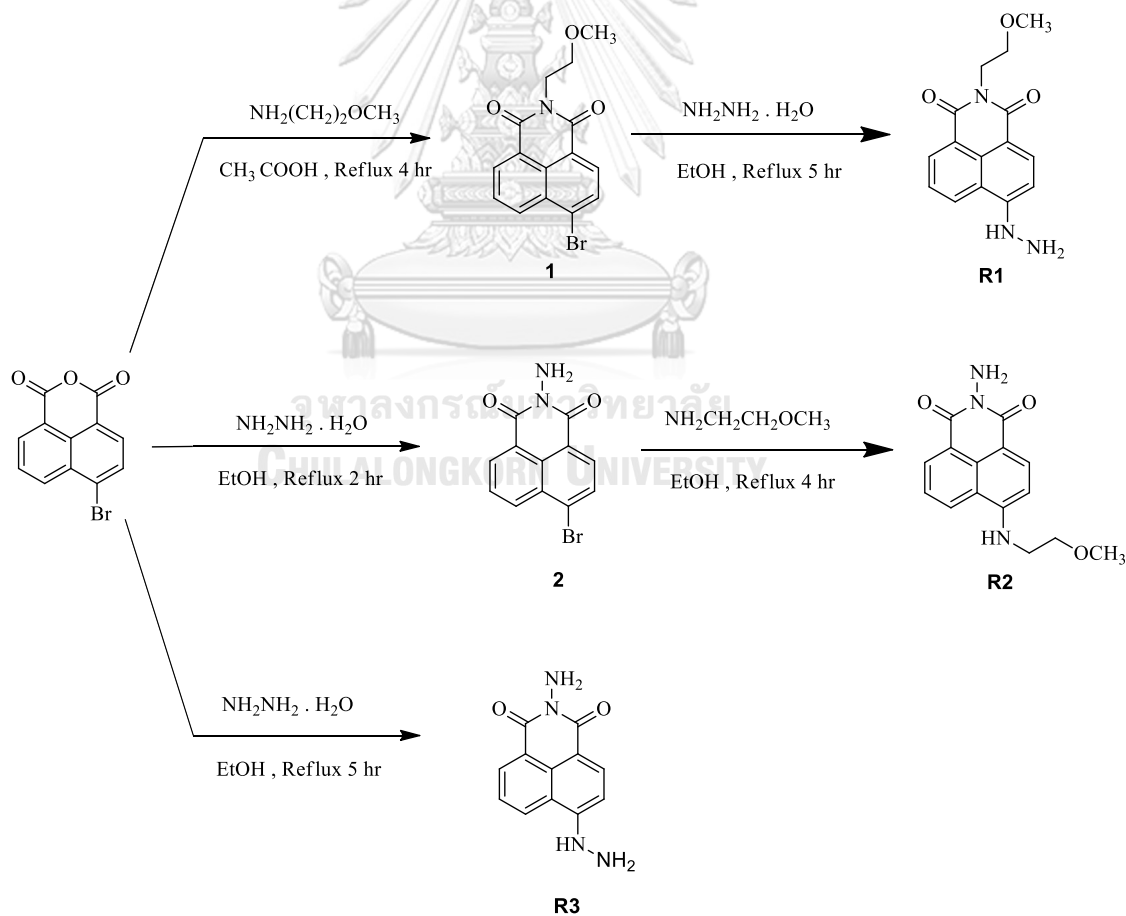
Scheme 3.1 Synthesis route of fluorophore **R1, R2, and R3**

The synthesis of **R1** began with a condensation of 4-bromo-1,8-naphthalic anhydride with 2-methoxyethylamine in acetic acid to afford intermediate **1**, followed by a nucleophilic substitution with hydrazine in ethanol to obtain **R1** in 87% yield. The ^{1}H NMR spectra of compound **1** to **R1** in DMSO-d_6 are shown in **Figure 3.1** All signals can be assigned as labelled in the structure. The characteristic signals include the amine proton (-NH) which appears as a broad singlet at 9.10 ppm, the amine proton (-NH$_2$) which appears as a singlet at 4.67 ppm, the two adjacent methylene protons (**f, e**) appearing as two triplets at 4.19 and 3.55 ppm and the methyl proton as sharp singlet at 3.25 ppm, respectively. The spectrum indicated a successful preparation of **R1** probe.
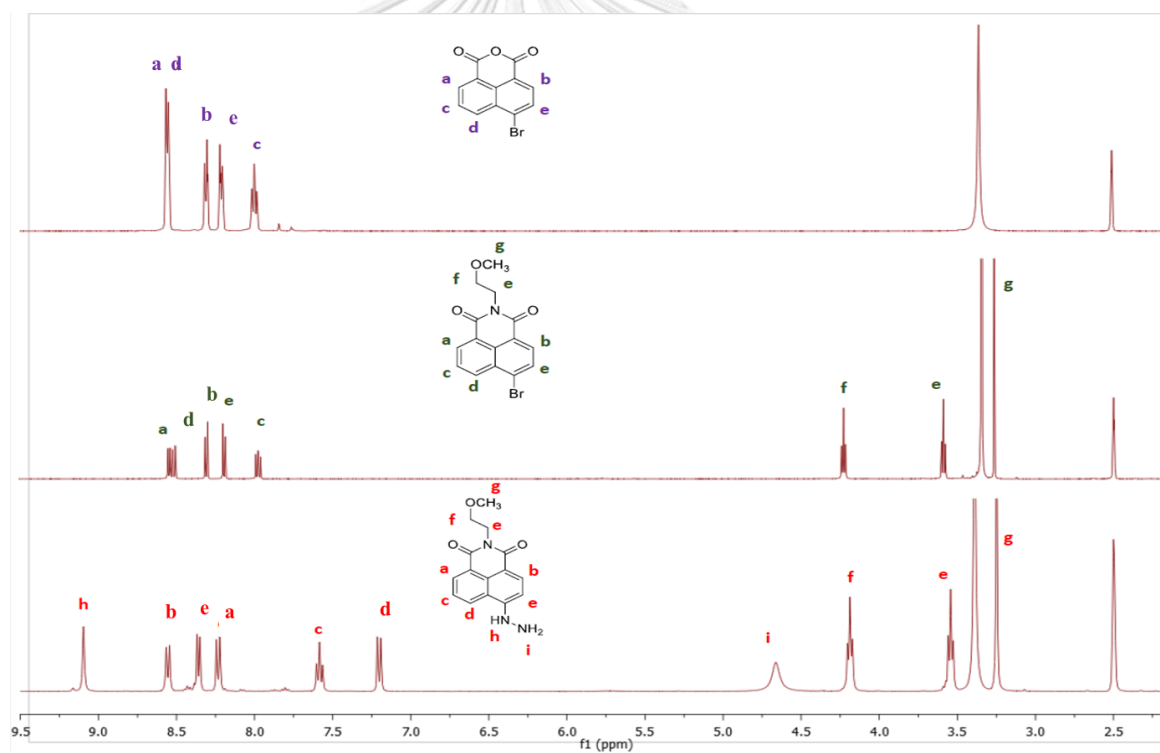
Figure 3.1 ^{1}H NMR spectra of compound naphthalic anhydride, **1**, and **R1** in DMSO-d_6

The synthesis of **R2** began with a condensation of 4-bromo-1,8-naphthalic anhydride with hydrazine hydrate in ethanol to obtain **2**, followed by a nucleophilic substitution with 2-methoxyethylamine in ethanol gave rise to **R2** in 60% yield. This lower yield of **R2** was probably caused by the unexpected formation of a by-product (**R3**) in the reaction of 4-bromo-1,8-naphthalic anhydride with hydrazine. The ^{1}H NMR spectra of compound **2** to **R2** in DMSO-d_6 are shown in **Figure 3.2.** All signals can be assigned as labelled in the structure. The characteristic signals include the amine proton (-NH) which appears as a triplet at 7.85 ppm, the two adjacent methylene protons (f, e) appearing as two triplets at 4.19 and 3.55 ppm and the methyl proton as a sharp singlet at 3.25 ppm, respectively.
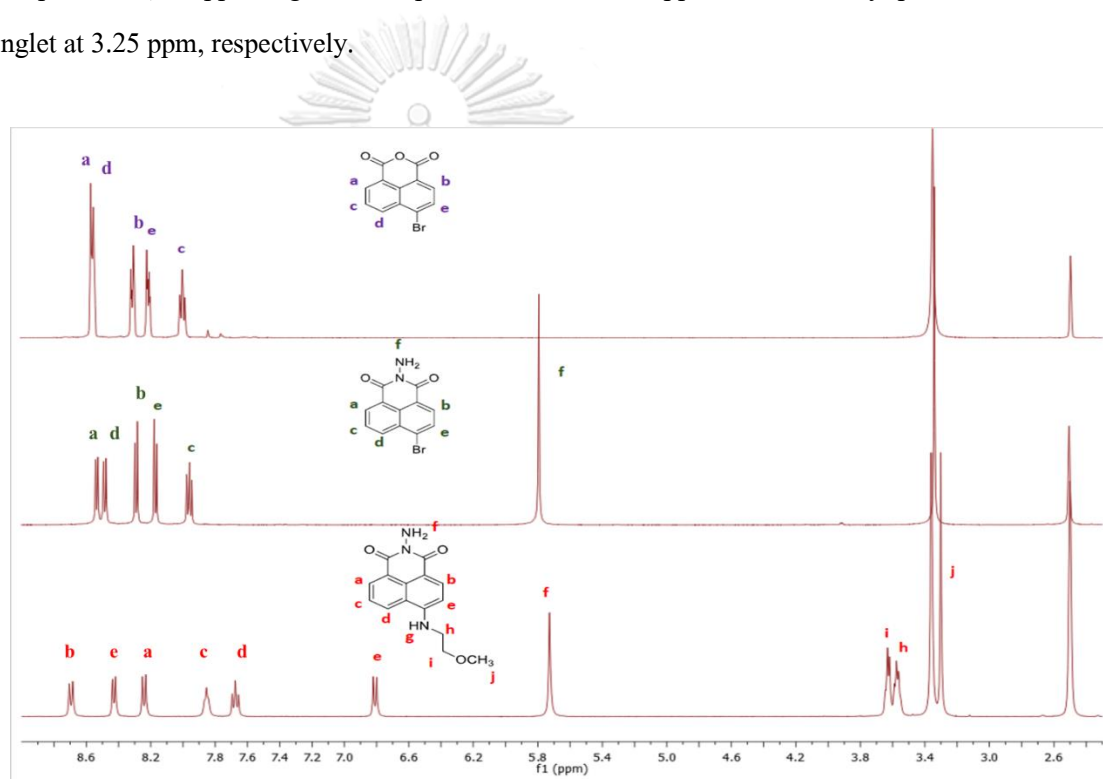
Figure 3.2 ^{1}H NMR spectra of compound naphthalic anhydride, **2**, and **R2** in DMSO-d_6

For the synthesis of **R3**, a one-pot reaction between 4-bromo-1,8-naphthalic anhydride and hydrazine hydrate in ethanol was performed and the product was obtaining in 90% yield. The ^{1}H NMR spectra of compound **R3** in DMSO-d_6 is shown in **Figure 3.3** All signals can be assigned as labelled in the structure. The characteristic signals include the amine proton (-NH) which appears as a broad singlet at 9.20 ppm, the two amine proton (-NH$_2$) which appears as a broad singlet at 5.72 and 4.69 ppm, respectively. The spectrum indicated a successful preparation of **R3** probe.
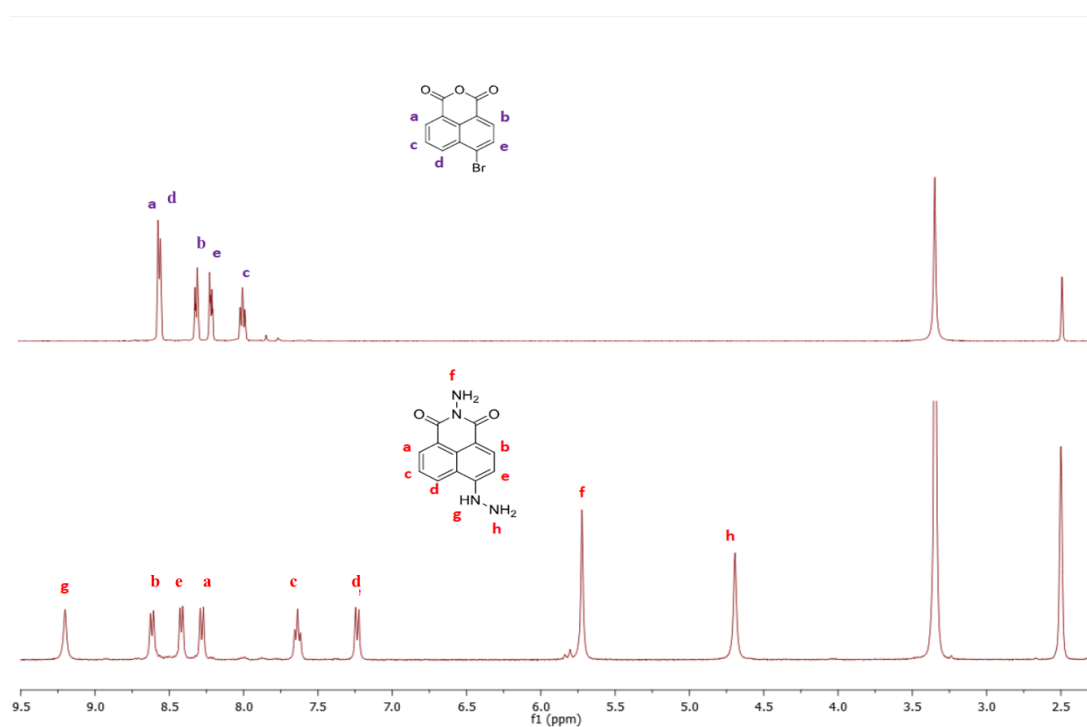
Figure 3.3 ^{1}H NMR spectra of compound naphthalic anhydride, **R3** in DMSO-d_6

Moreover, the molecular masses of **R1-R3** were determined by MALDI-TOF-MS (308.1001, 308.1006, 265.0695 respectively). The results are shown in **Figure 3.4** and also agreed with the calculated data.

	Compound	Compound + Na ion	Found
R1	285.1113	308.1011	308.1001

	Compound	Compound + Na ion	Found
R2	285.1113	308.1011	308.1006

	Compound	Compound + Na ion	Found
R3	242.0803	265.0701	265.0695
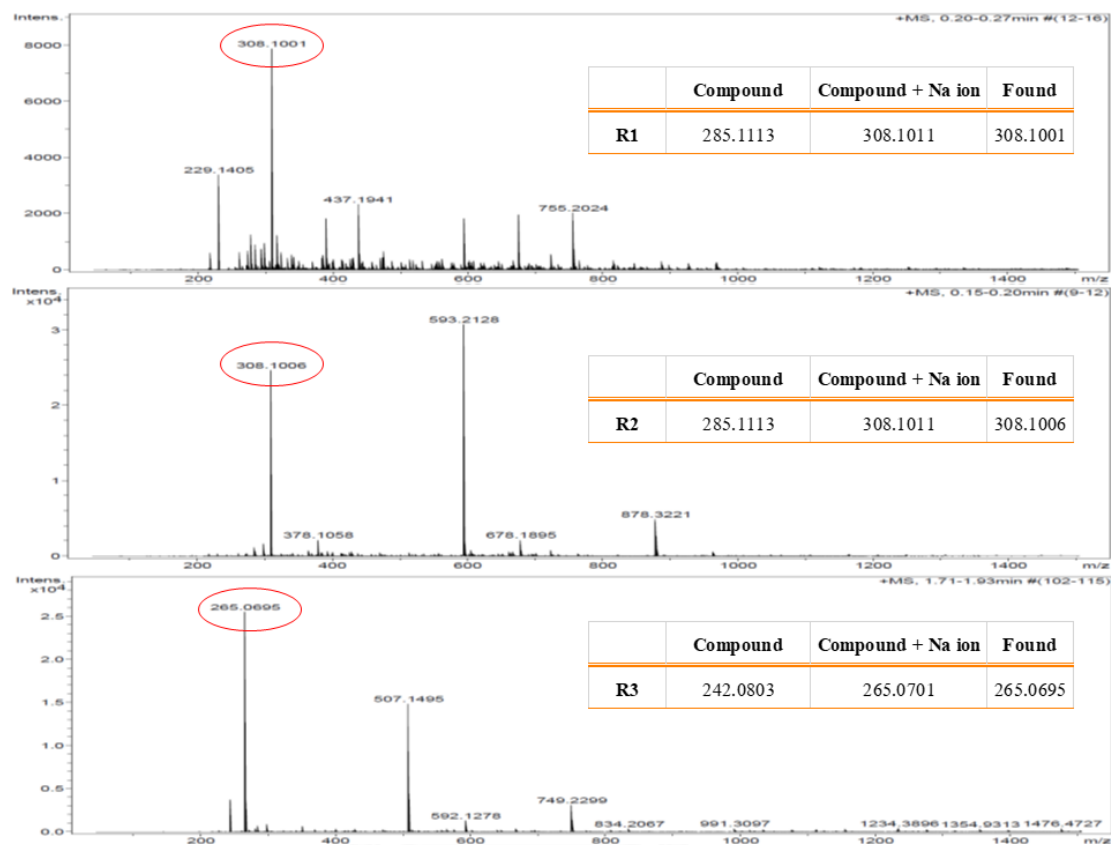
Figure 3.4 MALDI-TOF-MS spectra of **R1-R3**

3.2 Photophysical properties studies

The photophysical properties of **R1-R3** were investigated in DMSO. The photophysical properties are summarized in **Table 3.1**, while the UV-Vis and fluorescence spectra are shown **Figure 3.5**
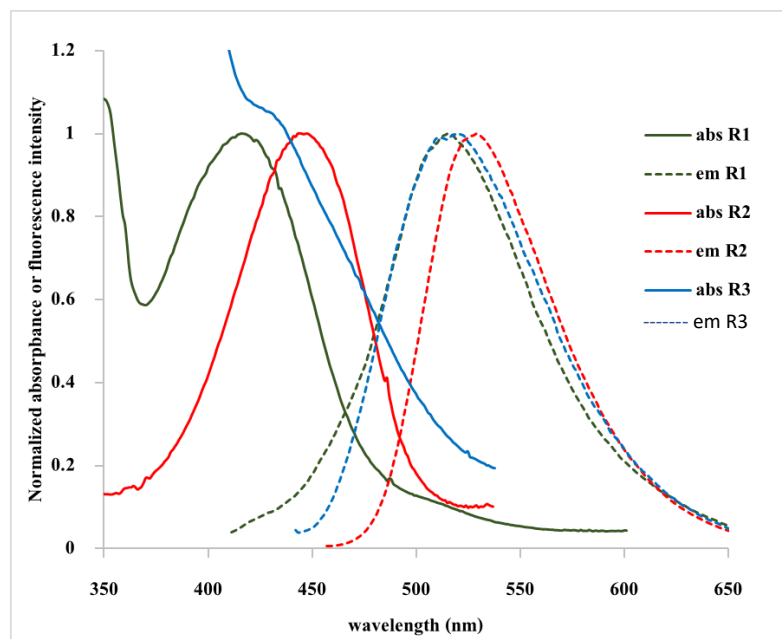
Figure 3.5 Normalized absorption and emission spectra of **R1-R3** in DMSO

The maximum absorption wavelengths appeared at 416, 447, and 440 nm for compounds **R1, R2** and **R3**, respectively. The molar extinction coefficients of these compounds were ranging between 6.4×10^3 and 9.7×10^3 M^{-1} cm^{-1}. The molar extinction coefficient for **R2** was significantly higher than the others because the substitution of 2-methoxyethylamino at the 4-position of naphthalimide may result in a more extensive conjugated system. Each fluorophore showed a single maximum emission wavelength at 515, 528 and 520 nm, respectively. This resulted in the green emission of **R1-R3** under the blacklight. The longest emission maxima in **R2** may result from the internal charge transfer from the electron-donating NH group to the electron-withdrawing naphthalimide C=O. The quantum efficiency of **R1-R3** were determined using quinine sulfate ($\Phi_F = 0.54$ in 0.1 M H_2SO_4) as standard. Each fluorophore showed the quantum efficiency with 0.1, 0.14 and 0.05 respectively. The lowest quantum yield of

R3 may result from the photo-induced electron transfer process from hydrazino group to the naphthalimide core.

Table 3.1 Photophysical properties of **R1-R3**

Compound	Absorption		Emision	
	λ_{max} (nm)	ε (M^{-1} cm^{-1})	λ_{max} (nm)	Φ^{a}
R1	416	6424	515	0.10
R2	447	9770	528	0.14
R3	438	8595	520	0.05

[a]Quinine sulfate in 0.1 M H$_2$SO$_4$ was used as the reference.

3.3 Selectivity screening of compound R1-R3

The sensing selectivities of **R1-R3** (10 μM) towards analytes (1 mM) such as formaldehyde, terephathaldehyde, naphthaldehyde, 3-methoxybenzaldehyde, 2-nitrobenzaldehyde, propionaldehyde, acetaldehyde, valeradehyde, and nonanal were also prepared in DMSO at 1 mM. In **Figure 3.6**, it was found that **R3** exhibited a substantial selective fluorescence enhancement in the presence of formaldehyde with a 4.5-folds fluorescence enhancement. The impressive sensitivity of **R3** towards formaldehyde may attribute to its lowest starting quantum yield, which can be enhanced upon a reaction between the hydrazino unit and formaldehyde. The formation of formaldehyde hydrazine could inhibit the photo-induced electron transfer, thus enhancing the emission signal. Meanwhile, the exceptional selectivity towards formaldehyde may result from its high reactivity in hydrazine formation with the sensor. Thus, further experiments will conducted using only **R3** probe.
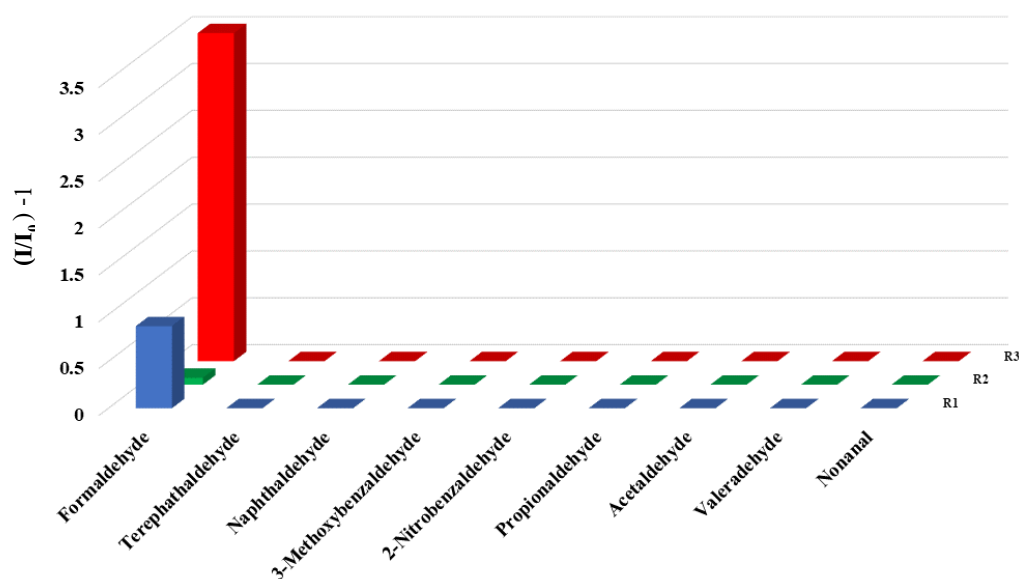
Figure 3.6 Fluorescence response of **R1-R3** (10 μM) towards various analytes (1.0 mM).

3.4 Propose mechanism

From the result above, the initial emission of **R3** in 5% acetic acid is weak due to PET process in which an excited electron is transferred from the donor (nitrogen lonepair) to the acceptor (naphthalimide fragment). The fluorescence intensity was enhanced after the addition of formaldehyde which resulted in the condensation reaction between hydrazine moiety and formaldehyde to generate an imine product **(Scheme 3.2)**. Upon the formation of this imine, the PET process was inhibited thus the fluorescence signal was enhanced.
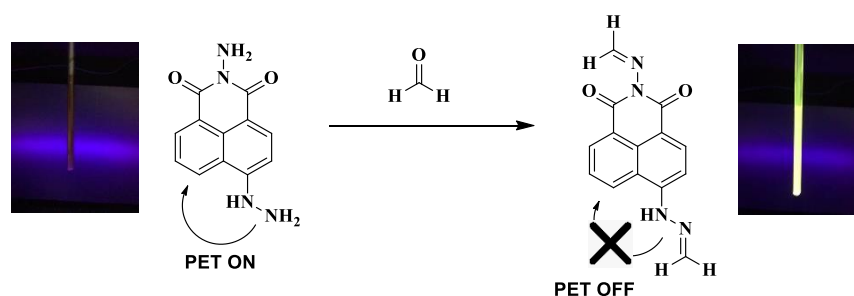
Scheme 3.2 Purposed sensing mechanism of **R3** toward formaldehyde

3.5 Effect of water content

The effects of solvent on emission of fluorophores were studied by varying the content of water in DMSO for a 10-μM solution of **R3** with 1 mM formaldehyde, as seen in **Figure 3.7**. The results showed that in high water content, **R3** fluorophores exhibited weak emission due to their poor solubility. However, it was decided that the use of 99 % water as the sensing media might be the optimum condition due to the lowest background fluorescent signal of **R3** and a good solubility of formaldehyde in water.
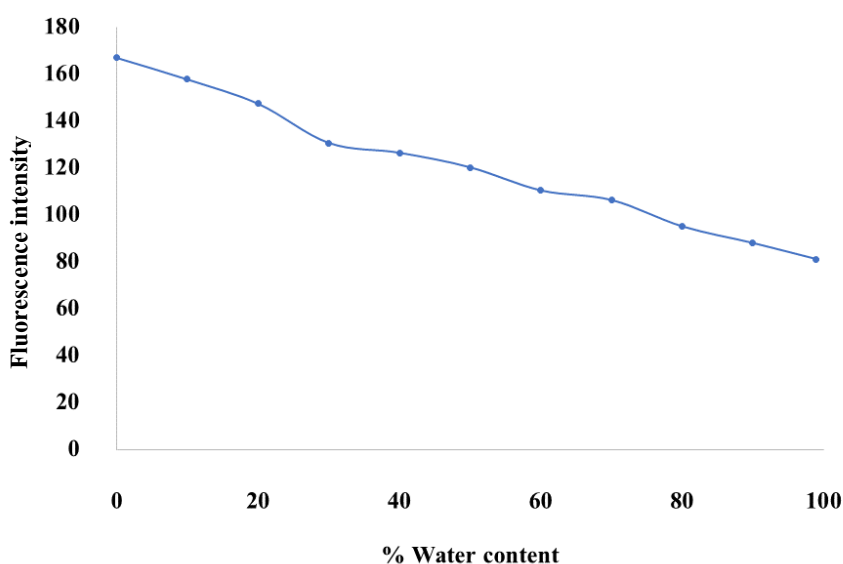
Figure 3.7 Fluorescence intensity of **R3** (10 μM) in DMSO mixed with DI water (10-99% v/v).

3.6 Effect of acidity and time dependent study

The fluorophore **R3** (10 μM) was tested under a pH range between 4.0 to 10.0 with 1 mM formaldehyde. The results were summarized in **Figure 3.8**. From this data, it was apparent that the background intensity of **R3** was unaffected under this pH range (blue dots). Upon the addition of formaldehyde, the fluorescent intensity increased at all pH (orange triangles). However, the fluorescent enhancement ratio (triangle/dot) were highest under the pH between 4 to 7). This information suggested that the reaction between probe **R3** and formaldehyde is more favorable under acid condition.
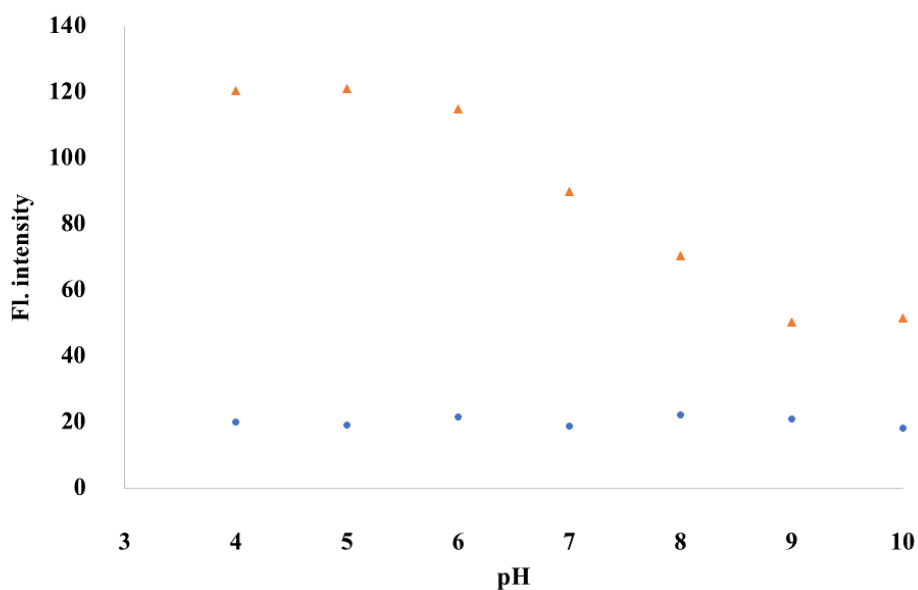
Figure 3.8 Effect of pH on the emission intensity of **R3** and their imine complexes.

The time dependent study of fluorescence response of **R3** to formaldehyde were test. Not only increase intensity ratio but also increase reactivity in acid condition. As you see from **Figure 3.9**. In DMSO the fluorescence response gradually increased during 0 – 60 min whereas in acid condition the reaction complete within 5 minute in 5% acetic acid. Therefore, we decide to use 5% acetic acid as the optimum condition for further study.

Figure 3.9 R3 in 5% acetic acid (left) and Time dependent changes in fluorescence intensity of **R3** in DMSO (right) (10 µM) upon addition of formaldehyde 100 equivalent.

3.7 Sensitivity of R3 toward formaldehyde

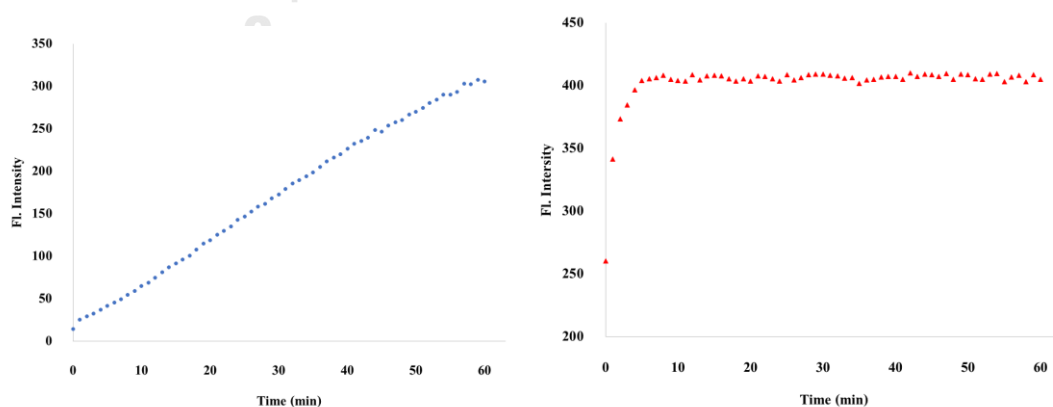With the optimized condition in hands, the absorption intensity in relationship with formaldehyde concentration was investigated upon the addition of various equivalent of formaldehyde (0 – 1 mM) in 5% acetic acid. For **R3** probe, the absorption peak at 420 nm doesn't change along with the increased concentration of formaldehyde. For fluorescence change, **R3** alone displayed weak fluorescence emission intensity at 520 nm (**Figure 3.10**). When we changed the addition of various equivalent of formaldehyde from 0 – 1 mM led to the fluorescence enhancement significantly. The strong green fluorescence emission was observed upon addition of formaldehyde with 4.5-folds fluorescence enhancement (**Figure 3.10**).
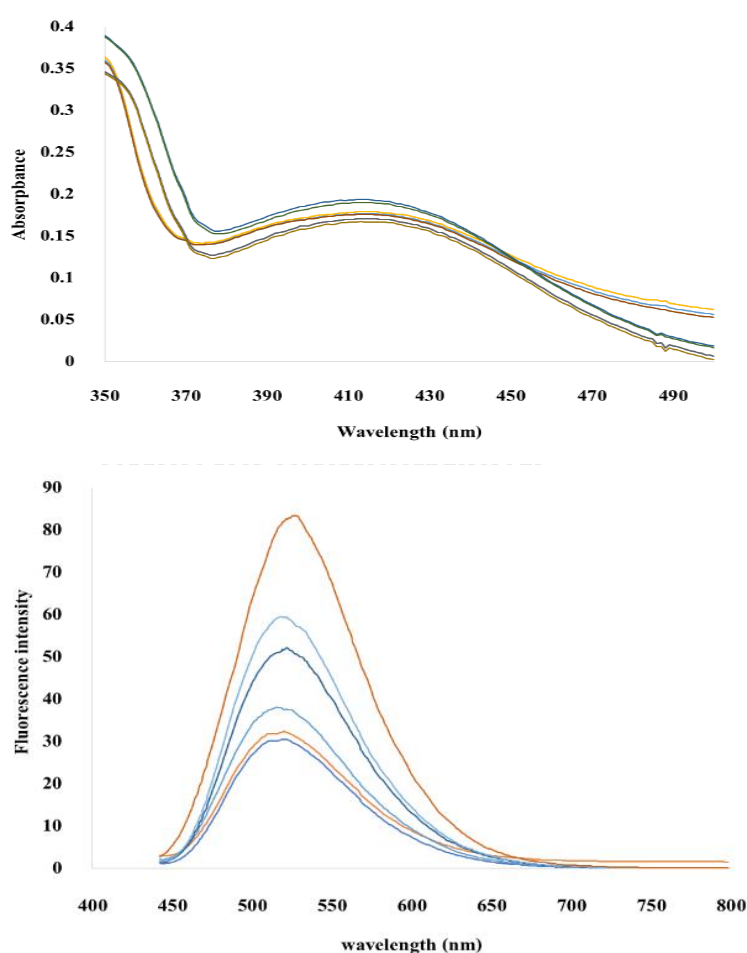

Figure 3.10 Absorption spectra change (left) and emission spectra change (right) of the solution of **R3** (10μM) upon addition of formaldehyde (1-100 eqiv) in 5% acetic acid.

3.8 Detection limit of R3 probe toward formaldehyde

The detection limit was calculated by the Eq. (DL = 3σ/m). In the Equation, σ is the standard deviation of blank measurement, which can be acquired by ten times measurements of emission spectrum of each sensor, m is the slope from plotting the fluorescence intensity versus formaldehyde concentrations in the range 0 – 1 mM. As shown in **Figure 3.11**, it shows a good linear relationship in the range of 0 to 1 mM for **R3** (R^2 = 0.9901). From above data, the detection limits at three-time noise was of 0.1 mM or 3.0 ppm. These values are lower than the WHO guideline (10 ppm) for formaldehyde allowed in fresh water. Therefore, **R3** is able to use for formaldehyde detection in aqueous system.
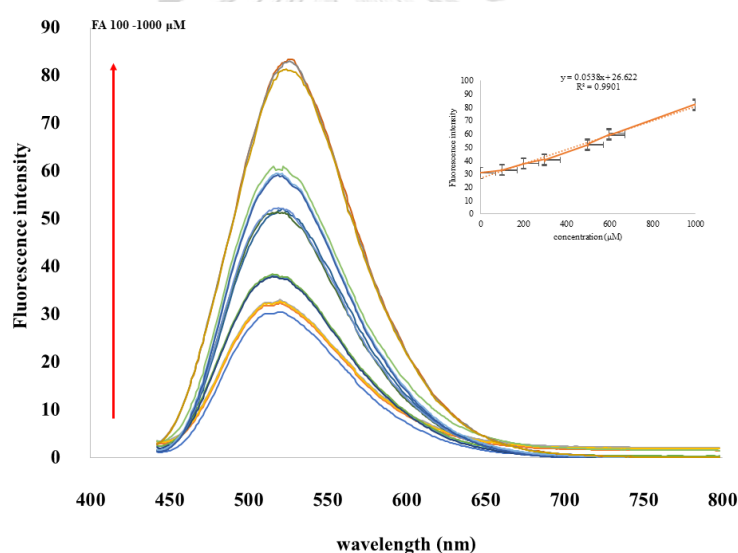
Figure 3.11 Fluorescence responses of **R3** (10 μM) towards formaldehyde (0.1-1.0 mM)

3.9 Interferent test

The interferent tests were conducted by adding several possible interferents to the mixture of **R3** and formaldehyde. The interferent samples such as terephathaldehyde, naphthaldehyde, 3-methoxybenzaldehyde, 2-nitrobenzaldehyde, propionaldehyde, acetaldehyde, valeradehyde, nonanal, sodium hydroxide, and glucose were selected due to their similar functional group and potential existence in food samples. The fluorescence responses (I_{FA+int}/I_{FA})

were summarized in **Figure 3.12**. The data indicated that none of the interferent sample could interfere the detection of formaldehyde even at a 10-fold concentration (**Figure 3.12**). This excellent selectivity may derive form a high reactivity and good water solubility of formaldehyde which lead to a complete conversion of hydrazine **R3** to its imine derivative.
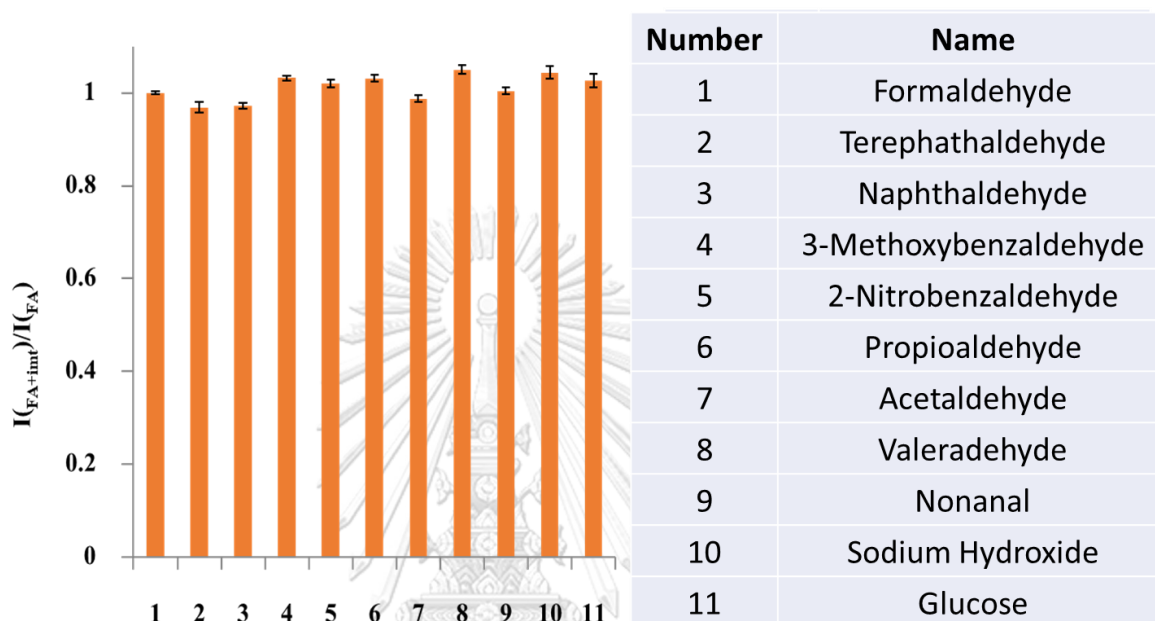

Number	Name
1	Formaldehyde
2	Terephathaldehyde
3	Naphthaldehyde
4	3-Methoxybenzaldehyde
5	2-Nitrobenzaldehyde
6	Propioaldehyde
7	Acetaldehyde
8	Valeradehyde
9	Nonanal
10	Sodium Hydroxide
11	Glucose

Figure 3.12 Fluorescence normalized responses of **R3** (10 μM) to the addition of formaldehyde (10 equivalent) mixed with various interferents (100 equivalent).

3.10 Method validation

To validate the use of **R3** probe as a sensor for formaldehyde in water, two types of water samples (Tap and DI water) were selected, spiked with formaldehyde (5 ppm), and analyzed for the amount of formaldehyde using traditional UV-Vis spectroscopic technique [25], [26] in comparison to our fluorescent sensor. Calibration curves for each method were constructed independently **(Figure 3.13)**, and the water sample were analyzed three times by each method. The analysis results in **Table 3.2** showed a good recovery of formaldehyde in both methods.
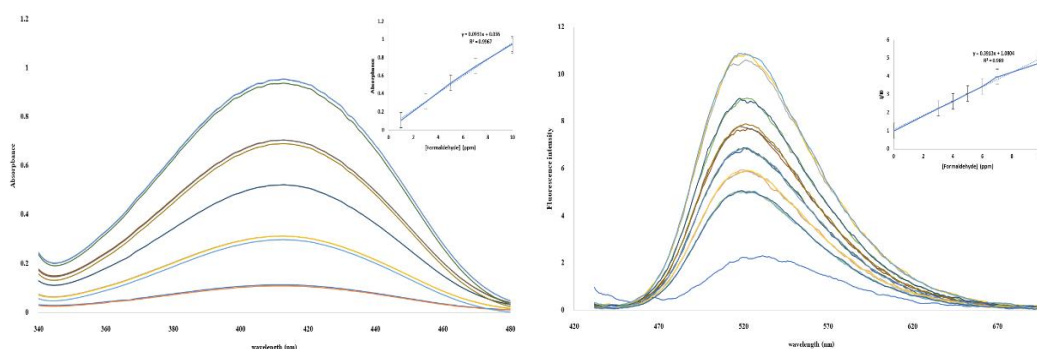
Figure 3.13 Absorption spectra of UV-Vis spectroscopic technique (left) and emission spectra of
fluorescent technique (right) upon addition of formaldehyde.

Table3.2 The recovery of formaldehyde in spectroscopic and fluorescent method.

Sample	Spectroscopic method		Fluorescent method	
	Found	% recovery	Found	% recovery
DI water spike 5 ppm	4.88 ± 0.064	97.5 ± 1.3	5.1 ± 0.3	102 ± 6.1
Tap water spike 5 ppm	4.98 ± 0.05	99.6 ± 1.1	4.95 ± 0.4	99 ± 8.1

3.10 Sensitivity enchancement for R3

From **Figure 3.5**, the signal enhancement ratio for R3 after the addition of formaldehyde
is around 3.5. In order to improve this sensitivity, the reduction of initial fluorescence signal of
R3 was attempted. The conversion of **R3** to its HCl salt was conducted by protonation of
hydrazine moiety with hydrochloric acid gas (**Scheme 3.3**). The resulting **R3-HCl** salt (**R3.HCl**)
was precipitate in THF. The structure of **R3.HCl** was confirm by ^{1}H NMR in DMSO-d_6 as shown
in **Figure 3.14 .** All signals can be assigned as labelled. In comparison to **R3**, the peaks of two -
NH_2 groups (4.7 and 5.7 ppm) transformed into a broad peak around 7 to 8 ppm which was a sign
of labile ammonium protons. In addition, the signal of proton **c** shifted slightly downfield due to
the electron-withdrawing nature of -NH_3^+ group.
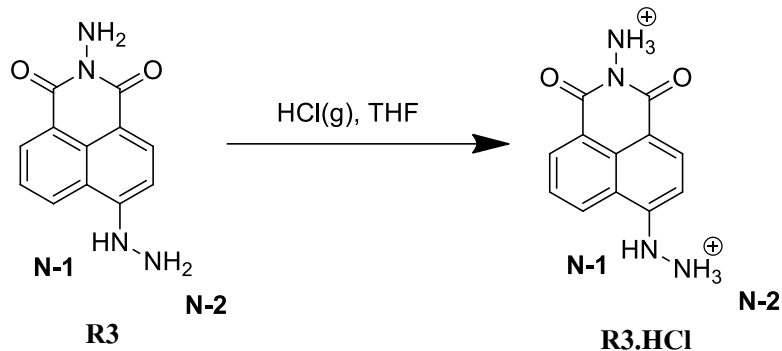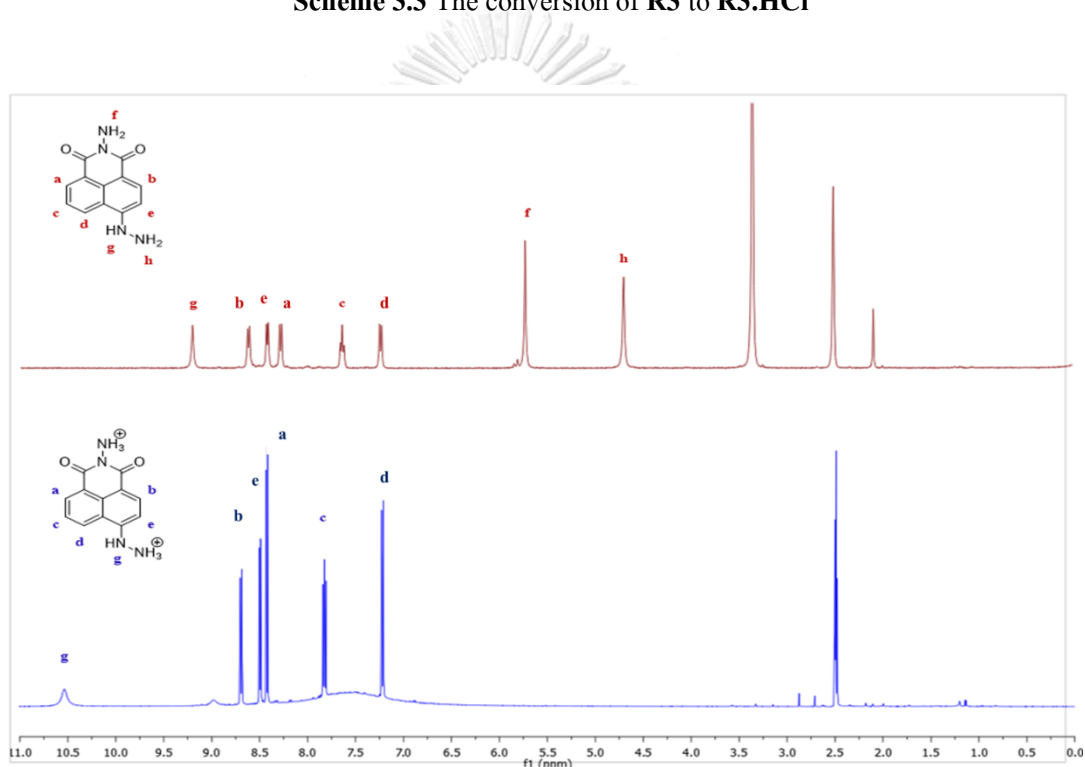
Scheme 3.3 The conversion of **R3** to **R3.HCl**

**Figure 3.14** ^{1}H NMR spectra of compound **R3** and **R3.HCl** in DMSO-d_6

In term of photophysical properties, **R3.HCl** possesses a longer absorption and emission maxima compared to **R3** (table). This may result from the higher electron-donating power of N-1 after protonation on N-2. On a similar scenario, the basicity of alkyl amine (R-NH$_2$) is generally higher than that of hydrazine (NH$_2$-NH$_2$) due to the highly electronegative neighboring nitrogen. Upon protonation on N-2, it would be more likely that there will be the delocalization of N-1 lone pair to the aromatic ring system. Therefore, the conjugated system in **R3.HCl** should be more

extended than that in **R3**, which may cause these spectral red shifts. Most importantly, the quantum yield decrease after the protonation (from 5 to 0.1%), which serve our intention to decrease the initial signal. This weaker emissive properties may result from the ICT process in which the N-1 lone pair electrons migrate to the aromatic ring and C=O unit (Scheme 3.4).

Table 3.3 Photophysical properties of R3 and R3.HCl

Compound	Absorption		Emission	
	λ_{max} (nm)	ε (M-1 cm-1)	λ_{max} (nm)	Φ_{a}(%)
R3	438	8,595	520	5
R3.HCl	455	12086	540	0.1

[a]Quinine sulfate in 0.1 M H_2SO_4 was used as the reference.
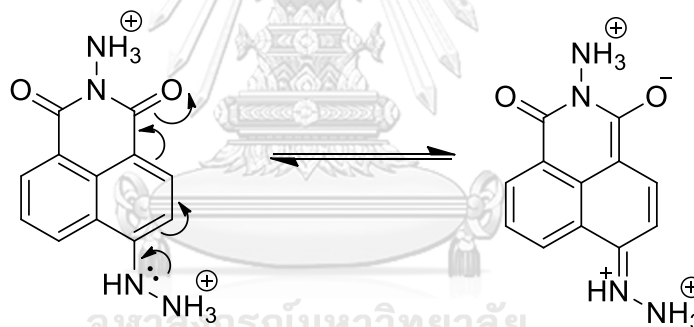
Scheme 3.4 The mechanism ICT process of **R3.HCl**

The intensity enchantment of **R3.HCl** was compared with **R3** in 5% acetic acid in the presence of 100 μM formaldehyde. As shown in **Table 3.3** and **Figure 3.15,** the enhancement ratio of **R3.HCl** was higher than **R3** (I/I_0 = 10 and 3.5, respectively). This probably due to the lower initial signal of **R3.HCl**.
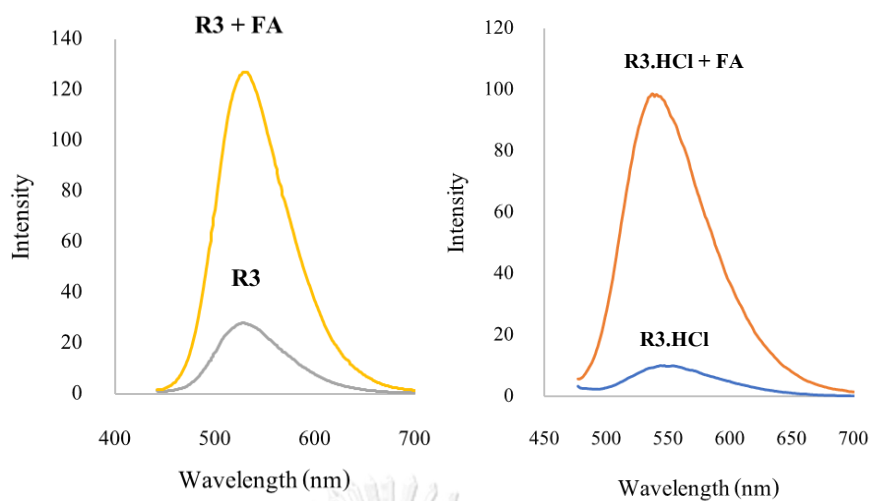
Figure 3.15 Fluorescence response of **R3** 10 µM (left) and **R3.HCl** 10 µM (right) toward 100 µM formaldehyde in 5% acetic acid.

The detection limit in **R3.HCl** was also calculated by the Eq. (DL = $3\sigma/m$). As shown in **Figure 3.16**, it shows a good linear relationship in the range of 0 to 250 µM for **R3.HCl** (R^2= 0.9952). From above data, the detection limits at three-time noise was of 4.7 µM. These values are lower than **R3**. Not only does the protonation of **R3** increase enhancement ratio, it could also lower the LOD for the formaldehyde detection.
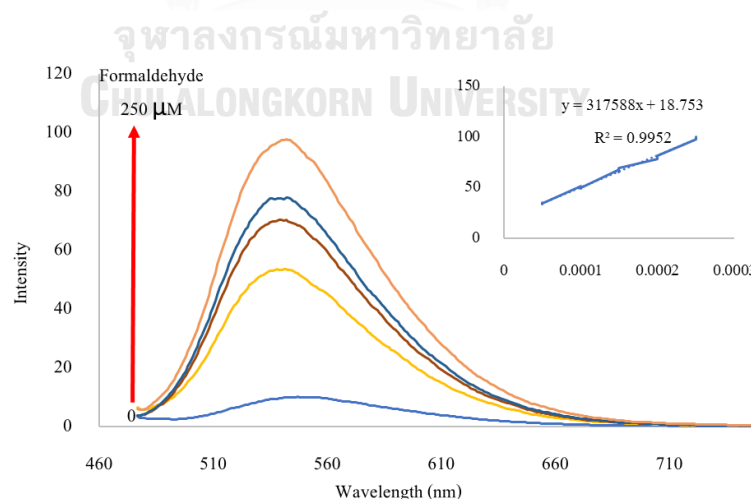

Figure 3.16 Fluorescence responses of **R3.HCl** (10 µM) towards formaldehyde (0 - 250 µM).

3.11 Fabrication of sensor in sol gel

Silica sol gel are generally used as a microporous support matrix in which fluorophores are entrapped and into which analyte species may diffuse and interact. The used of this process on **R3.HCl** sensor can be quite interesting because of the hydrophilic nature and suitable optical properties of silica sol gel. For this purpose, we prepared a stock solution composing of TEOS, ethanol, and H_2O in a mole ratio of 1:1:2, respectively. To a 50-mL portion of this stock solution, a few drops of concentrated HCl were added and the mixture was stirred and stored in the refrigerator (4ºC). This stock sol gel precursor was then pipetted into vials (500 µL each) then a stock solution of **R3.HCl** was added in order to obtain a final mixture containing 100 µM of **R3.HCl**. After allowing the TEOS to undergo acid-catalyzed hydrolysis and evaporation of water at room temperature for overnight, a sol gel based sensor for formaldehyde was obtained. The IR spectrum of sol gel and modified sol gel were shown in **Figure 3.17.** The characteristic peak of sol gel (Si-O-Si, Si-OH) was still observed in sol gel modified. Under the irradiation of black light, a weak emission was detected in the modified sol gel, which indicate the existence of **R3.HCl**. After adding formaldehyde solutions (20 M to 0.02 µM) to this modified sol gel, A strong yellow fluorescence could be observed under black light (**Figure 3.18**). These results suggested a feasibility to fabricate **R3.HCl** as Sol-Gel fluorescent sensor for detection of formaldehyde in aqueous samples.
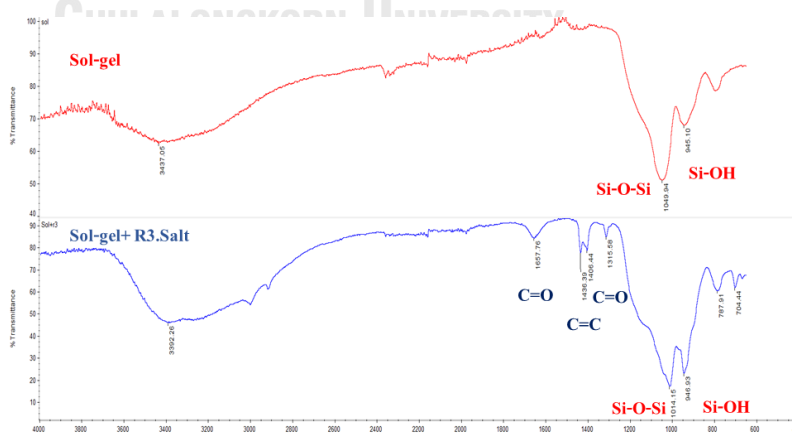

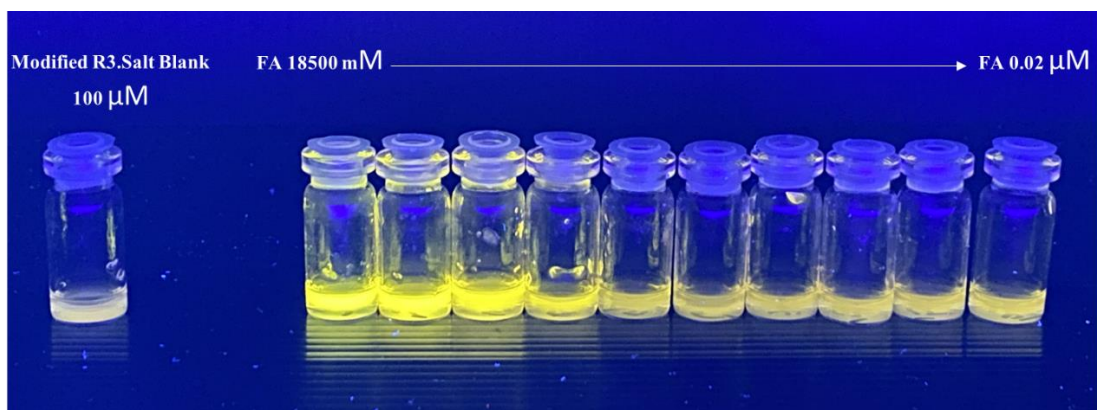**Figure 3.17** The IR spectrum of sol gel and modified sol gel

Figure 3.18 Fluorescence image of modified sol gel with 100 μM **R3.HCl** upon adding

formaldehyde 20 M to 0.02 μM.

3.12 Optimization of sol gel modification

According to the WHO guideline, the allowable amount of formaldehyde in drinking water should not exceed 10 ppm or 0.3 mM. From the result in Figure 3.18, it is possible to adjust the concentration of **R3.HCl** in order to tune the sensitivity for formaldehyde sensing. Two sets of sol gel sensors were prepared with **R3.HCl** at 10 and 1 μM and tested with formaldehyde solution of various concentrations (2 mM to 0.02 μM). From **Figure 3.19** it was apparent that the sol gel sensor derived from 10 μM of **R3.HCl** could distinguish the formaldehyde solution at 2 and 0.02 μM, while the sensor with 1 μM of R3.HCl could only detect formaldehyde at 2 mM.

Figure 3.19 Fluorescence image of modified sol gel with 10 μM of **R3.HCl** upon adding
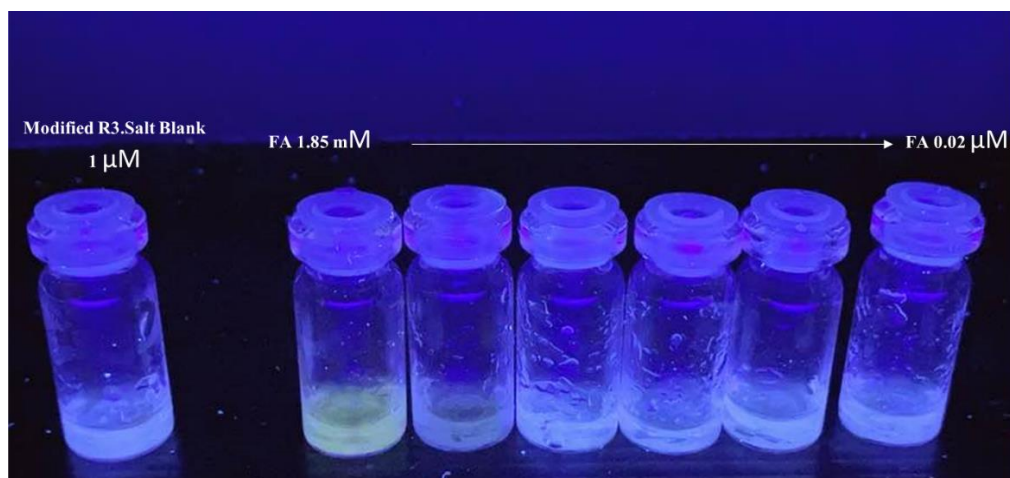
formaldehyde 2 mM to 0.02 μM.

Figure 3.20 Fluorescence image of modified sol gel with 1 μM **R3.HCl** upon adding

formaldehyde 2 mM to 0.02 μM.

CHAPTER IV

CONCLUSION

In summary, three fluorophores (**R1, R2** and **R3)** were successful synthesized from the condensation reaction and nucleophilic replacement of the hydrazino ($-NHNH_2$) and the 2-methoxyethylamino groups ($-NHCH_2CH_2OCH_3$) into the naphthalimide core. Only **R3** probe can be used as a naked eye sensor displaying highly selective and sensitive emissive change from non-fluorescence to green fluorescence in the presence of formaldehyde. The detection limit of **R3** probe was calculated to be 0.1 mM or 3 ppm which are below the allowable concentration set by WHO in drinking water. The sensing mechanisms of **R3** probe involved the reaction between hydrazine moiety and formaldehyde to generate imine product. Other aldehydes and related analysts did not show significant interference in fluorescence spectrum. Moreover, the sensitivity of **R3** probe toward formaldehyde was successfully enhanced by protonation of the hydrazine moiety with HCl gas to give **R3.HCl**. In solution phase, the detection limit of **R3.HCl** probe was calculated to be 4.7 µM which was 20 times lower than that of **R3**. In addition the fabrication of **R3.HCl** in sol gel was successfully demonstrated. The doping of 10 µM of **R3.HCl** in silica sol gel led to a sensor which was capable of formaldehyde detection at 2 to 0.02 µM by naked eyes.

REFERENCES

1. Organization, W.H., *Concise international chemical assessment document 40: Formaldehyde.* Geneva: World Health Organization, 2002.

2. De Groot, A.C. and M. Veenstra, *Formaldehyde‑releasers in cosmetics in the USA and in Europe.* Contact Dermatitis, 2010. **62**(4): p. 221-224.

3. Yeasmin, T., et al., *Present status of marketing of formalin treated fishes in domestic markets at Mymensingh district in Bangladesh.* International Journal of Biological Research, 2010. **1**(4): p. 21-24.

4. Kerns, W.D., et al., *Carcinogenicity of formaldehyde in rats and mice after long-term inhalation exposure.* Cancer research, 1983. **43**(9): p. 4382-4392.

5. Aalto‑Korte, K., et al., *Occupational contact allergy to formaldehyde and formaldehyde releasers.* Contact Dermatitis, 2008. **59**(5): p. 280-289.

6. Saiki, R., et al., *Brain infarction correlates more closely with acrolein than with reactive oxygen species.* Biochemical and biophysical research communications, 2011. **404**(4): p. 1044-1049.

7. OLSENA, J.H. and M. DØSSING, *Formaldehyde induced symptoms in day care centers.* American Industrial Hygiene Association Journal, 1982. **43**(5): p. 366-370.

8. Wahed, P., et al., *Determination of formaldehyde in food and feed by an in-house validated HPLC method.* Food Chemistry, 2016. **202**: p. 476-483.

9. Shin, H.S. and H.H. Lim, *Simple determination of formaldehyde in fermented foods by HS‑SPME‑GC/MS.* International journal of food science & technology, 2012. **47**(2): p. 350-356.

10. Španěl, P., et al., *Analysis of formaldehyde in the headspace of urine from bladder and prostate cancer patients using selected ion flow tube mass spectrometry.* Rapid communications in mass spectrometry, 1999. **13**(14): p. 1354-1359.

11. Wang, X., et al., *Functionalized nanoporous TiO2 fibers on quartz crystal microbalance platform for formaldehyde sensor.* Sensors and Actuators B: Chemical, 2012. **171**: p. 658-665.

12. Jameson, D.M., *Introduction to fluorescence*. 2014: CRC press.

13.   De Silva, A.P., T.S. Moody, and G.D. Wright, *Fluorescent PET (Photoinduced Electron Transfer) sensors as potent analytical tools.* Analyst, 2009. **134**(12): p. 2385-2393.

14.   Silva, A.P., *Recent evolution of luminescent photoinduced electron transfer sensors. A review.* Analyst, 1996. **121**(12): p. 1759-1762.

15.   Bruemmer, K.J., T.F. Brewer, and C.J. Chang, *Fluorescent probes for imaging formaldehyde in biological systems.* Current opinion in chemical biology, 2017. **39**: p. 17-23.

16.   Brewer, T.F. and C.J. Chang, *An aza-cope reactivity-based fluorescent probe for imaging formaldehyde in living cells.* Journal of the American Chemical Society, 2015. **137**(34): p. 10886-10889.

17.   Song, H., et al., *A tailor designed fluorescent 'turn-on'sensor of formaldehyde based on the BODIPY motif.* Tetrahedron Letters, 2012. **53**(37): p. 4913-4916.

18.   Lee, Y.H., et al., *A biotin-guided formaldehyde sensor selectively detecting endogenous concentrations in cancerous cells and tissues.* Chemical Communications, 2016. **52**(75): p. 11247-11250.

19.   Fu, Y., et al., *Synthesis and fluorescent property study of novel 1, 8-naphthalimide-based chemosensors.* Molecules, 2018. **23**(2): p. 376.

20.   Dong, B., et al., *A rapid and facile fluorimetric method for detecting formaldehyde.* Sensors and Actuators B: Chemical, 2016. **222**: p. 325-330.

21.   Tang, Y., et al., *Lysosome-targeted turn-on fluorescent probe for endogenous formaldehyde in living cells.* Analytical chemistry, 2016. **88**(19): p. 9359-9363.

22.   Melde, B.J., B.J. Johnson, and P.T. Charles, *Mesoporous silicate materials in sensing.* Sensors, 2008. **8**(8): p. 5202-5228.

23.   Montoya, L.A. and M.D. Pluth, *Selective turn-on fluorescent probes for imaging hydrogen sulfide in living cells.* Chemical Communications, 2012. **48**(39): p. 4767-4769.

24.   Jiang, S.-Q., et al., *Rational design of a highly sensitive and selective "turn-on" fluorescent sensor for PO 4 3⁻ detection.* Dalton Transactions, 2015. **44**(48): p. 20830-20833.

25.   Rohyami, Y. and R.M. Pribadi. *Validation of methods on formalin testing in tofu and determination of 3, 5-diacetyl-dihydrolutidine stability by UV-Vis spectrophotometry.* in *AIP Conference Proceedings.* 2017. AIP Publishing LLC.
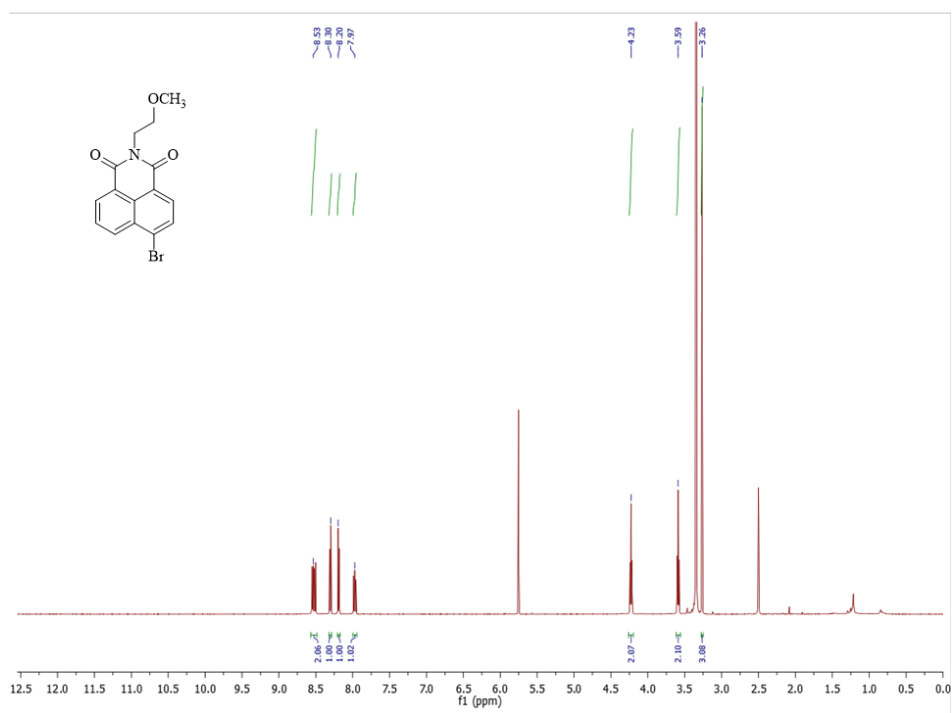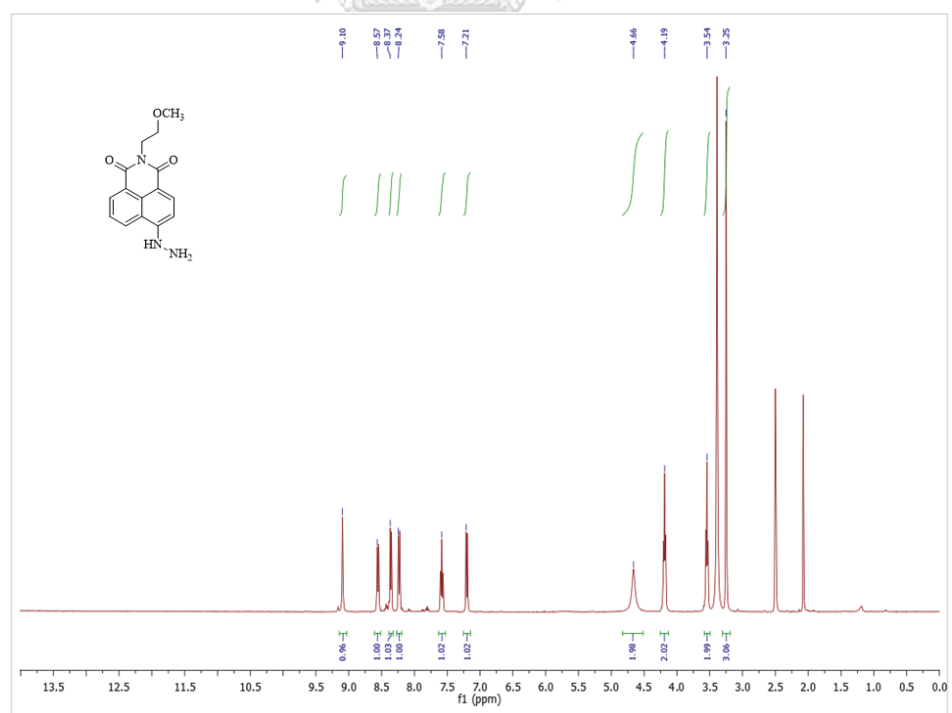
26.   Smith, R.V. and P.W. Erhardt, *Nash determination for formaldehyde in the presence of bisulfite.* Analytical Chemistry, 1975. **47**(14): p. 2462-2464.

APPENDIX

Figure S.1 ^{1}H NMR spectra of **(1)** in DMSO-d_6

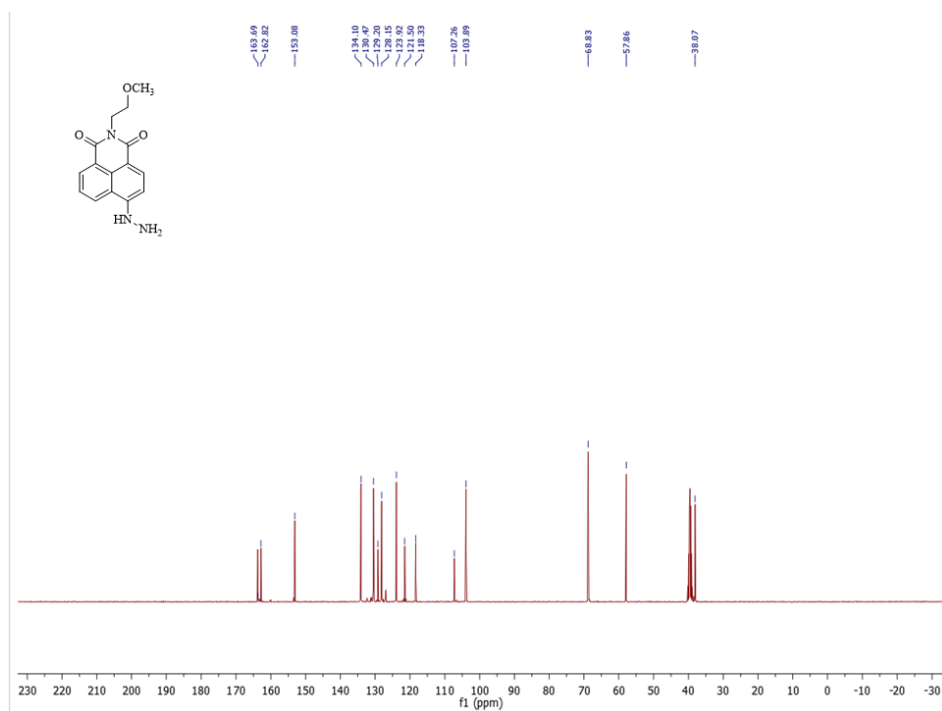**Figure S.2** ^{1}H NMR spectra of **R1** in DMSO-d_6

Figure S.3 ^{13}C NMR spectra of **R1** in DMSO-d_6
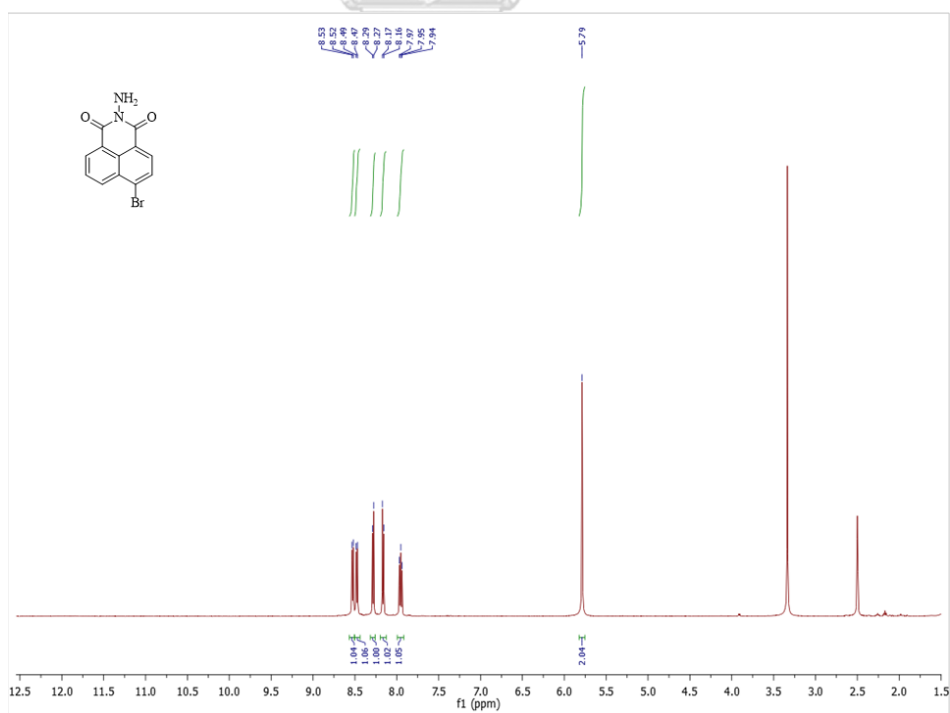
Figure S.4 ^{1}H NMR spectra of **(2)** in DMSO-d_6
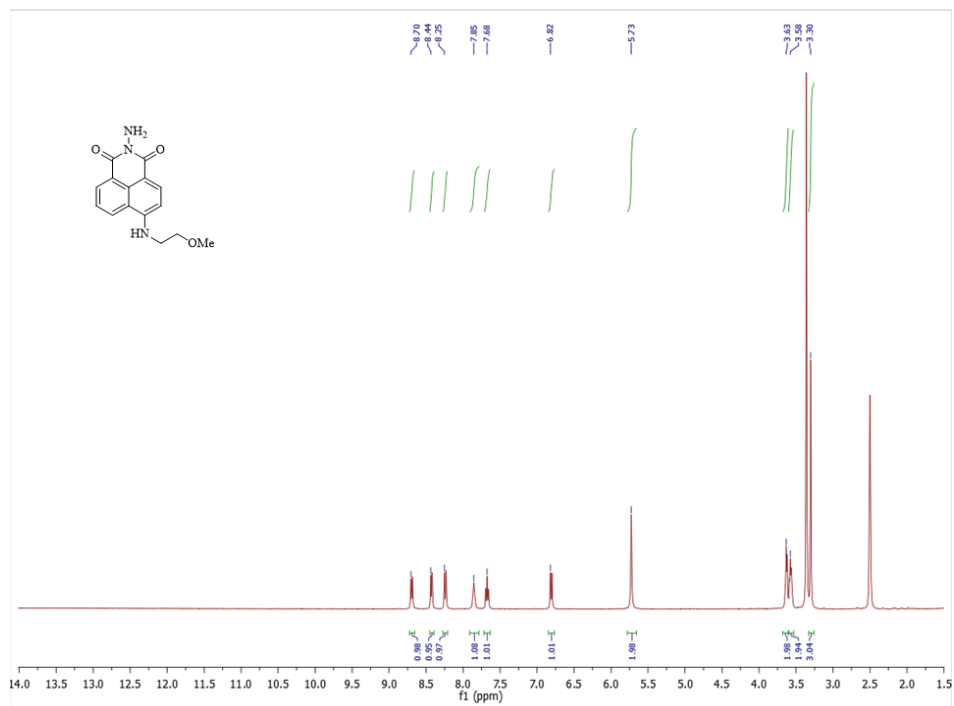
Figure S.5 ^{1}H NMR spectra of **R2** in DMSO-d_6
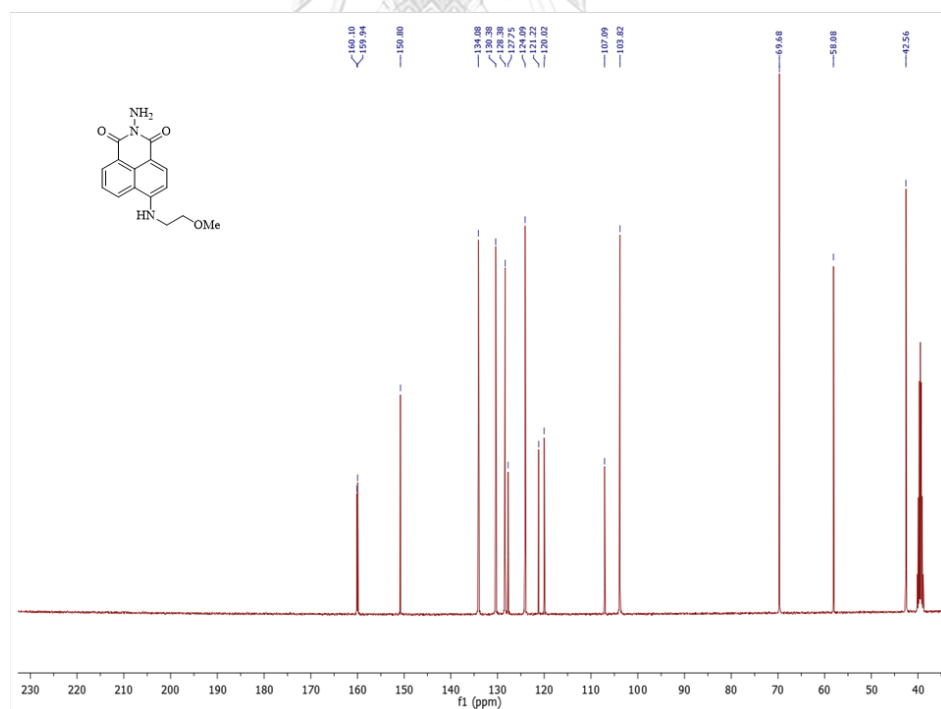
Figure S.6 ^{13}C NMR spectra of **R2** in DMSO-d_6
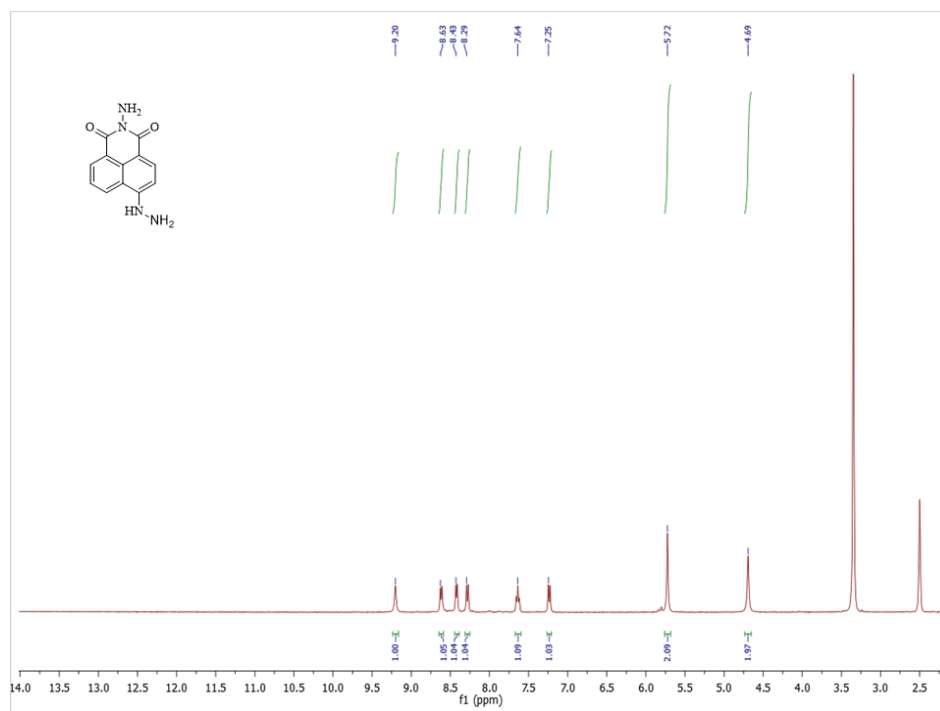
Figure S.7 ^{1}H NMR spectra of **R3** in DMSO-d_6
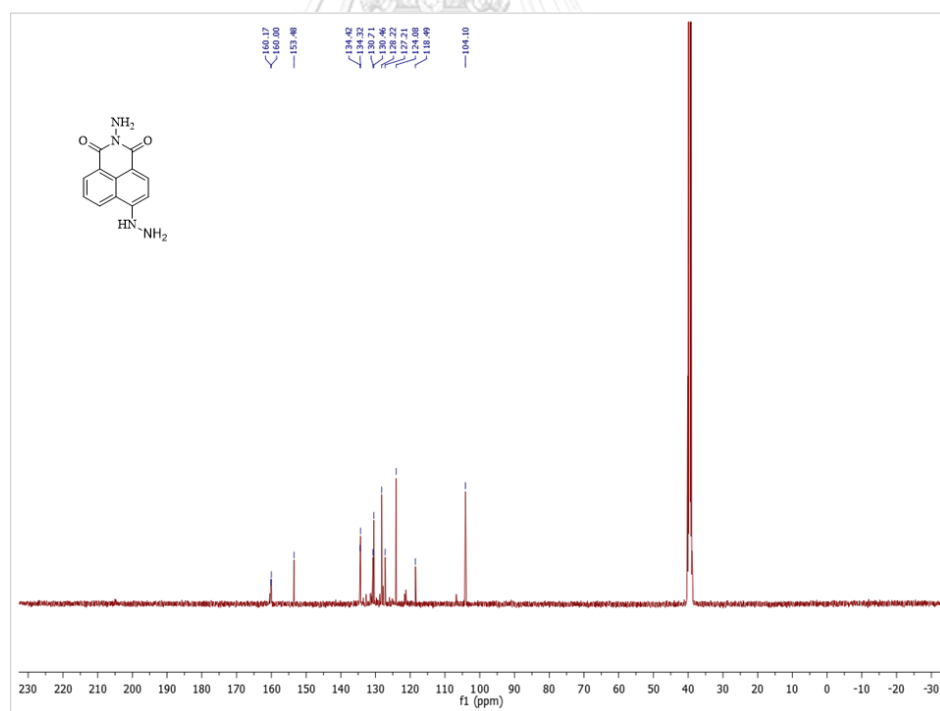
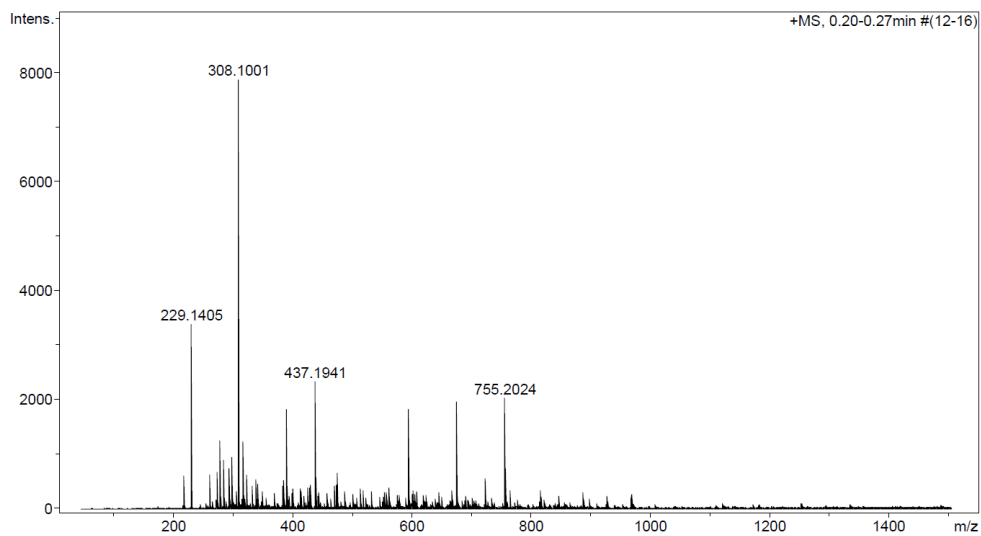**Figure S.8** ^{13}C NMR spectra of **R3** in DMSO-d_6
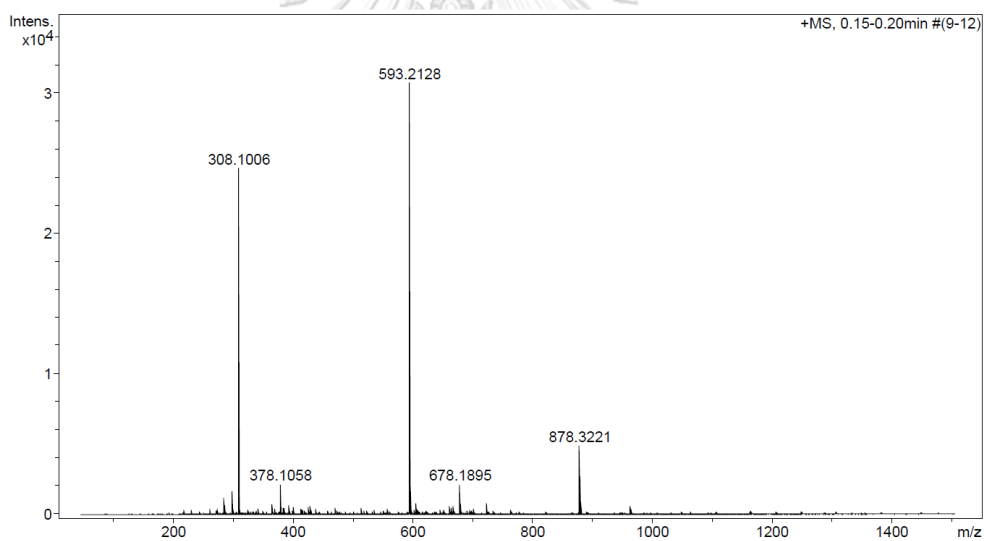
Figure S.9 MALDI-TOF-MS spectra of **R1**
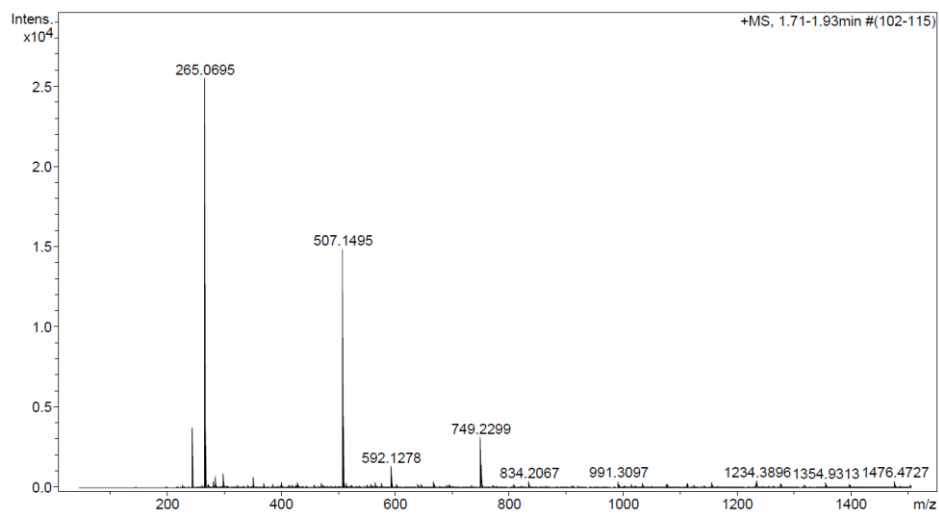

Figure S.10 MALDI-TOF-MS spectra of **R2**

Figure S.11 MALDI-TOF-MS spectra of **R3**
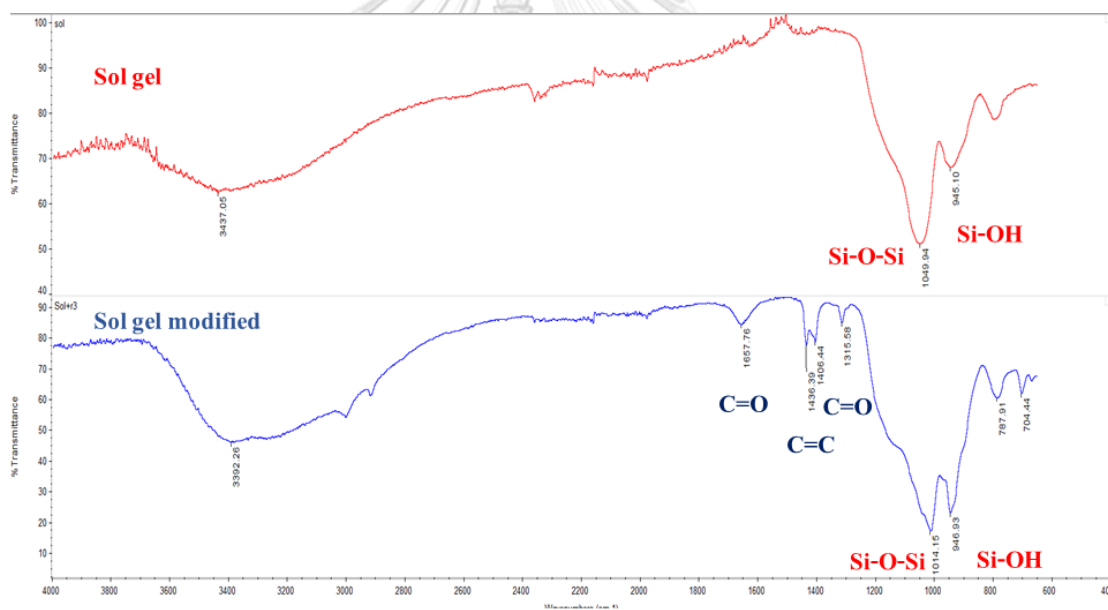
Figure S.12 The IR spectrum of sol gel and modified sol gel

VITA

NAME	Apicha Maharat
DATE OF BIRTH	04 Feb 1990
PLACE OF BIRTH	Bangkok
INSTITUTIONS ATTENDED	Thammasat university
HOME ADDRESS	111/448 M.3 Bannd Bangtorad Bangtorad sub-district Muang district Samutsakorn 74000
PUBLICATION	-
AWARD RECEIVED	-

จุฬาลงกรณ์มหาวิทยาลัย

CHULALONGKORN UNIVERSITY